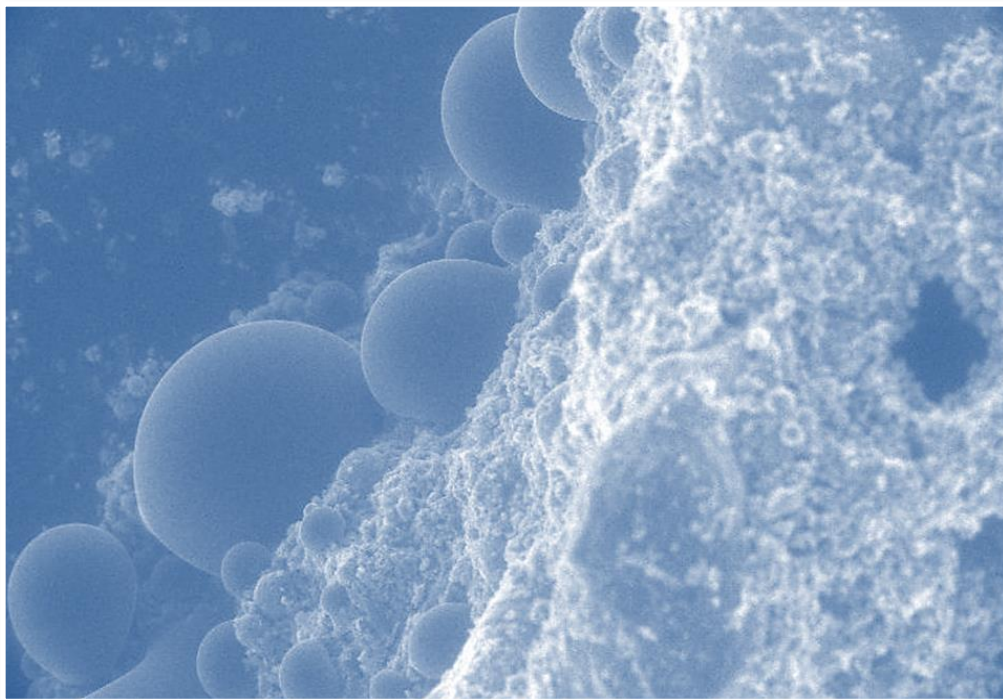


University of Pécs

Breuer Marcell Doctoral school

Faculty of engineering and information technology



in cooperation with Hochschule Wismar
University of Applied Science, Technology, Business and Design
Faculty of engineering

Thesis Booklet of the dissertation of Peter Körber M.Sc.

to obtain the degree
Philosophiae Doctor Ph.D.

at the Breuer Marcell Doctoral school
University of Pécs

Proof of the effectiveness of water-repellent injection methods for a subsequent masonry seal, based on experimental investigations on bricks and mortar, with the scanning electron microscope in ESEM mode, as well as in the correlation to conventional detection methods

Abstract

Due to the problem of rising masonry moisture on capillary masonry in the absence of a cross-section sealing, injection agents that have a hydrophobic and pore-filling effect, subsequently are used in the borehole method. Such a subsequent masonry sealing must be checked for effectiveness. In addition to already existing macroscopic methods, a new microscopic detection method is presented in this work. This detection method uses ESEM technology in the SEM to generate and detect in situ dew processes at samples taken from the injection level of the examined masonry. The output of the results is done by image or film. By means of the condensation with the medium of water, the contact angle measurement method on the dew drops can be used to make accurate statements about the water-repellent capabilities of the examined sample and thus about the sealing success.

There are detectable correlations to the macroscopic detection methods. In the presently presented new detection method, the procedure is carried out in two stages by capturing macroscopic data, related to the injection medium used in stage 1. In the second stage, microscopic contact angles are measured in the ESEM by means of condensation processes and correlated with the data obtained in stage 1 using a mathematical model. As a result, a geometric, qualitative and quantitative picture of the capillarity changed by the use of the injection agents can be presented.

The method presented in this work is a further development of already existing methods and offers the advantage to have very small samples and to be investigated in a short time with very precise results. The new detection method is suitable for practical use.

1. CONTENT

1.	CONTENT	1
2.	INTRODUCTION AND TASK	2
2.1	INTRODUCTION INTO THE TOPIC	2
3.	REFLECTION TO THE 4 THESES	4
3.1.1	Thesis 1	4
3.1.1.1	Question: To what extent does the subsequent sealing level prevent the capillary forwarding after the injection? ...	4
3.1.1.2	To thesis 1	7
3.1.2	Thesis 2	9
3.1.3	Thesis 3	9
3.1.3.1	ESEM condensation: hydrophilic properties => water film formation	10
3.1.3.2	ESEM condensation: hydrophilic properties => Contact angle < 90°	10
3.1.3.3	ESEM condensation: hydrophobic properties => Contact angle > 90°	11
3.1.3.4	ESEM condensation: super hydrophobic properties => Contact angle > 150°	11
3.1.3.5	ESEM condensation: Contact angle measurement with the 'Geometric Drop Contour Analysis'	12
3.1.4	Thesis 4	13
3.1.4.1	Results of the investigations in stage 1	14
3.1.4.2	Evaluation of the macroscopic measurement results	15
3.1.4.3	Investigations at stage 1a (RH- measurements)	17
3.1.4.4	Results of the data logger measurement at stage 1a	17
3.1.4.5	Investigations in the ESEM at stage 2	18
3.1.4.6	ESEM contact angles, correlated W-values, RH-values	18
3.1.4.7	Correlations to the ESEM- contact angles	18
3.1.4.8	Mathematical modelling	18
3.1.4.9	Matrix of the new test procedure	21
4.	CONCLUSION, POSTGRADUATE RESEARCH INTERESTS	21
4.1	CONCLUSION	21
4.2	POSTGRADUATE RESEARCH INTERESTS	22
1.	APPENDIX	23
I.	PUBLICATIONS OF P. KÖRBER IN THE CONTEXT OF THIS THESIS	23
II.	REFERENCES	23
III.	LIST OF FIGURES	26
IV.	TABLE LIST	27
V.	DIAGRAM DIRECTORY	27
VI.	CONSULTATIONS	28
VII.	STATUTORY DECLARATION	28
VIII.	NOTE OF THANKS	28
IX.	CURRICULUM VITAE	29
2.	LIST OF ATTACHMENTS	30

2. INTRODUCTION AND TASK

2.1 Introduction into the topic

In the refurbishment of old buildings, especially in the area of monuments [1], massive masonry walls consisting of brick masonry [2] are found very often. Since brick is a capillary-active building material [3], there is a pronounced water absorption and release as well as water transport behaviour on the walls of old buildings [1], [4], [5], [6], [7], [8]. Although already known from antiquity, the regular use of functioning building waterproofing began in Europe around 1890. Nevertheless, there were no uniform rules for the execution of structural waterproofing at that time. Only in the 1930s structural waterproofing was normatively regulated in parts of Europe. Although the cross-section sealing in massive walls had already a higher priority than other sealings on buildings at the end of the 19th century, in Europe cross-section sealings were regularly installed in masonry walls since 1930 onwards [15]. In the old building area, very often buildings to find that have a cellar, even if the space requirements made this cellar unnecessary. This is related to the previous construction / use, in which the basement was due to lack of sealing technology while permanently moist, but served as a 'buffer' to the upper floors, which thereby could be kept sufficiently dry. In this way the buildings were built without a cross-sectional sealing. For these reasons solid brick walls in cellars are often encountered in old building renovation and monument preservation, in which there is rising masonry moisture due to non-existent cross-sectional sealings. Due to usage or reuse and value retention requirements, however, there is a great need in the renovation of old buildings and in the preservation of monuments to seal capillary masonry walls permanently against increasing humidity in the wall cross-section [9], [10].

In the retrofitting of masonry cross-section seals there are three main groups. On the one hand, mechanical cross-section seals can subsequently be installed by means of wall sawing methods. On the other hand, the missing sealing membrane can be supplemented as part of a wall replacement procedure. However, each method means mechanical and thus static interventions in the old substance. Therefore the largest group of cross-section sealings is represented by the masonry injection methods contemplated herein, which do not require static interventions [11], [12], [13].

There are currently about 150 different injectables available in Europe [62] for the subsequent cross-sectional sealing of capillary masonry. All injectables have in common that they are applied by the production of borehole chains in the masonry. The injectables react chemically. The sealant layer in the masonry is physically formed [14], [15], [16].

There are non-pressurized processes which are applied by capillarity or by gravity. There are also pressurized processes in which the injection medium is pressed into the masonry under low or medium pressure. Due to the inhomogeneities inherent in the bricks used at that time, which may result, for example from differences in the fire, difficult conditions are often encountered at old bricks.

In addition, there are any previous processing errors of the mortar joints, war damage, cracks and any cavities of the masonry to be treated. Although the condition of the old masonry, when treated with injectables in the masonry diagnostics, is to be investigated before the injection agent is used, there are still imponderables, since the defects in the masonry are usually concealed and therefore may go unnoticed [17], [18], [19].

The basic efficacy of an injection can be demonstrated in Europe through WTA certification. However, this evidence refers to a standard masonry with standard mortar and is tested in the laboratory on test specimens in a long-term procedure. Other known detection methods are based on laboratory tests on specimens and local long-term measurements of the drying behaviour after the application of injection media. Therefore, there are no statements on the efficacy of the local on-site injection so far, which can be provided in a short time with small amounts of samples [20], [21], [22].

There is a need for a suitable new detection method. The use of injectables by means of borehole chains has the goal of changing the capillarity of the old masonry structure in such a way that, according to the previously formulated sealing aims, the capillary transport of water in the masonry is slowed down or even stopped [23], [24], [25], [26], [27], [28].

In order to be able to monitor the injection procedure and to be able to demonstrate the effectiveness of the injection medium, it is therefore necessary to record the quality and quantity of capillarity that actually changed on the object. In addition, the geometric spread of the applied injection agent in the masonry must be checked, as this is directly related to the effectiveness of the injection. Since all existing detec-

tion methods have a long-term procedure and take place on laboratory test specimens, these test methods cannot be used for practical purposes defined here [29], [30], [31], [32], [33], [34], [35], [36], [37].

In this work a new detection method for the qualitative and quantitative detection of modified capillarity by application of injectables is presented. This procedure complies with the requirements set out in 3.1.4. The intention of the verification procedure presented here, is to develop the existing procedures further. The detection method presented in this work is based on the contact angle determination in the Environmental Scanning Electron Microscope, ESEM. The ESEM is a modified version of a scanning electron microscope, SEM. In contrast to the SEM, the ESEM can be used in low-vacuum mode. This circumstance allows the supply of a medium (here water steam) under the investigation. A cooling table in the chamber allows the sample to be cooled while the air in the chamber is at 100% relative humidity. By changing the chamber pressure a condensation can be provoked in the ESEM [38], [39], [40], [41], [42], [43].

The contact angles can be determined on the resulting drops of water. When measuring the contact angle, one makes use of the interfacial tension of the water. Both static contact angles and dynamic contact angles can be measured in the ESEM. The contact angles provide information about the capillarity of the sample material on which the drop has formed [44], [45], [46], [47], [48], [49], [50]. In this work, the geometric drop contour analysis was developed for the contact angle measurement in the ESEM, where the drops in space can be measured using a geometric model, see Fig. 11. The detection method presented here was demonstrated by a 2 - stage test on 122 mortar and bricks samples treated with injection agents. In the first stage, conventional macroscopic measurement procedures were performed on the samples for data collection. In the second step, microscopic contact angle measurements were taken on a selection of samples, in addition to the measurement of RH values measured in sealed chambers in the middle of the samples, with using the ESEM. Use of a mathematical modelling, the data obtained in the first stage could be correlated with the contact angles measured in the ESEM in the second stage. In this way, the first-stage macroscopic values such as w-values and fictitious water contents can be assigned to the ESEM measurement values. As a result, in addition to the ESEM contact angles, mathematically determined w-values and fictitious water contents for the respective sample are obtained, which provide information about the changed capillarity in comparison to the reference sample. The w-values can be evaluated according to the existing evaluation matrix, Fig. 1 [51], [15]. The fictitious water contents and the RH-values can be processed in a moisture simulation. In the case of application, samples are taken depth-separated in measuring axes in a pre-defined measuring field, to be examined for their contact angles in the ESEM. From the data obtained from this, a geometrically differentiated picture of the altered capillarity of the masonry is given in correlation with the data of the stage 1. The new detection method can provide information on the quality of the inserted injection medium as well as on the basis of the geometric assignment which also provides information about the quantity of injection agent application.

$w \geq 2.0 \text{ kg/m}^2 \text{ h}^{0.5}$	strongly absorbent
$w \leq 2.0 \text{ kg/m}^2 \text{ h}^{0.5}$	water resistant
$w \leq 0.5 \text{ kg/m}^2 \text{ h}^{0.5}$	water repellent
$w \leq 0.001 \text{ kg/m}^2 \text{ h}^{0.5}$	waterproof

Figure 1: Evaluation matrix of the results of the W-Value measurements, based on DIN EN 15148 and DIN EN 1062 T3

Source: J. Weber, Bauwerksabdichtung in der Altbausanierung p. 38 [15]

3. REFLECTION TO THE 4 THESES

3.1.1 Thesis 1: Due to anomalies in the building material and in the masonry, laboratory screening on laboratory test specimens to proof the capillarity of building materials, treated with injections, analogous to the WTA certificate, is not meaningful alone. Quality and efficacy monitoring of specimens, taken from the object, are required

3.1.1.1 Question: To what extent does the subsequent sealing level prevent the capillary forwarding after the injection?

If the subsequent sealing produced by certified injection media fails in capillary masonry, the following causes basically exist:

- The masonry has a too high moisture content and (or) excessively high degree of salinity for the selected injection medium and (or) the selected injection process
- The borehole distances have not been selected correctly
- The spreading of the injection is geometrically irregular

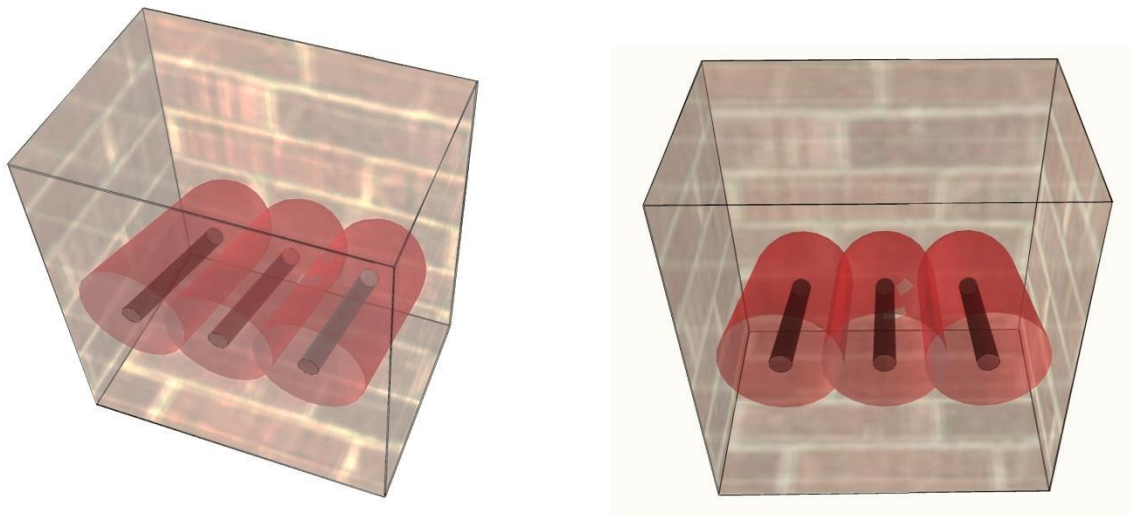


Figure 2: Application spread and borehole distances are ideal:
=> overlapping cylindrical spread, Source: Körber, P.

[52], [53], [54], [55], [56]

In the following sketched 3 cases is presented, where the basic question about the changed capillarity in the injection level is explained. It can be seen in Fig. 2 that the spreading of the injection medium applied via the borehole chain has taken place in such a way that the areas changed in their capillarity (here illustrated ideally in cylindrical form) sufficiently overlap (intermesh). In this case there is:

- a sufficient spread of the injection agent in the masonry and
- a right borehole distance and
- a sufficient spreading geometry

The result is a 'sealing area' in the masonry. The planned sealing quality can be achieved.

In Fig. 3 it can be seen that the spreading of the injection medium applied via the borehole chain has taken place in such a way that the areas changed in their capillarity (also shown here ideally in cylindrical form) do not sufficiently overlap. In this case there is:

- an insufficient spreading of the injection agent in the masonry and (or)
- an incorrect borehole distance and (or)
- an insufficient spreading geometry

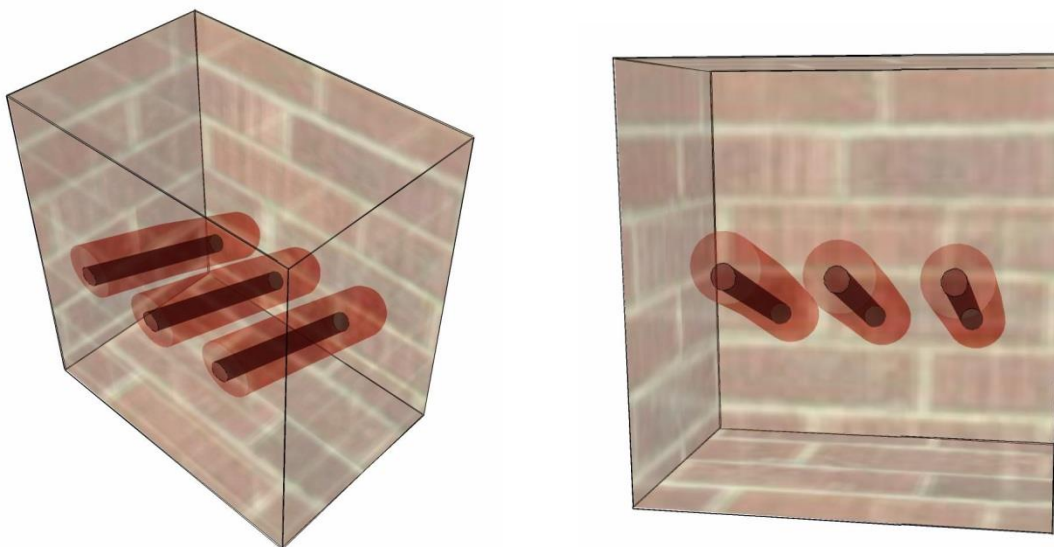


Figure 3: The spread of the injection application is too small / borehole distances are too far, there is a cylindrical injection spread, but it is not overlapping, Source: Körber, P.

As shown in Fig. 3, there is no complete sealing area in the masonry. The sealing quality, as shown in Fig. 2, can only be achieved partially. Causes for the non-uniformly changed capillarity in the sealing area are here either the insufficient spread of the injection medium itself and (or) the too great distance of the selected boreholes.

In fact, however, geometrically deformed injection spreads have often been observed on subsequently sealed objects and also on samples treated with injections. These are shown schematically in Fig. 4. It can be seen in Fig. 4 that the spread of the injection medium applied via the borehole chain has taken place in such a way that the areas changed in their capillarity are not uniform and that they are geometrically deformed. In addition, the areas do not overlap sufficiently. In this case there is:

- a non-uniform and insufficient spreading of the injection agent in the masonry and (or)
- an incorrect borehole distance and (or)
- a geometrically unknown, diffuse spread geometry

There is no complete 'sealing area' in this masonry here as well. Here the sealing, as shown in Fig. 2, can only be achieved partially. In the pictures shown in Fig. 5, the asymmetrical, geometrically deformed spread at injection-treated bricks that have been separated in the borehole area, has been identified. The hydrophobic areas of the brick halves are outlined in black. The remaining areas of the brick halves are hydrophilic. The deformed spreading of the injection agent, commonly found on brick walls, is due to causes inherent in the masonry material and the workmanship.

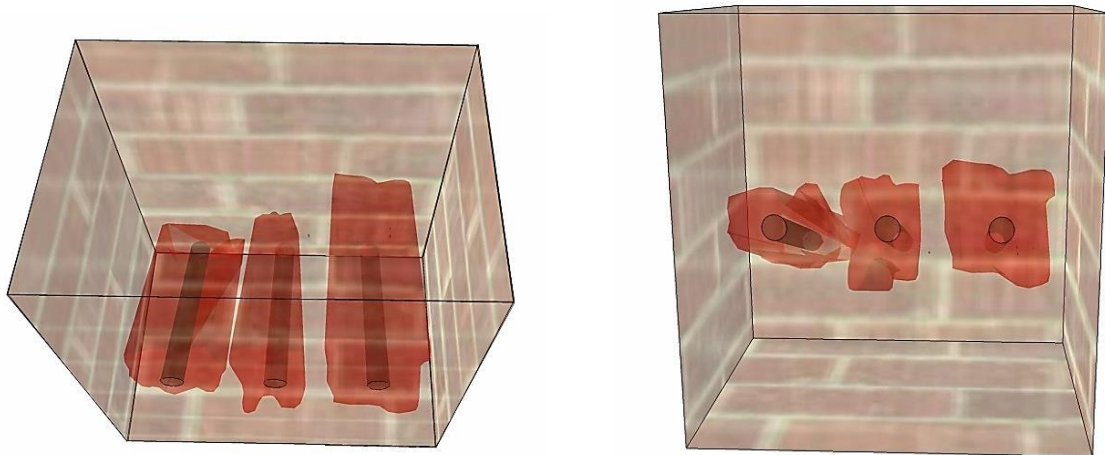
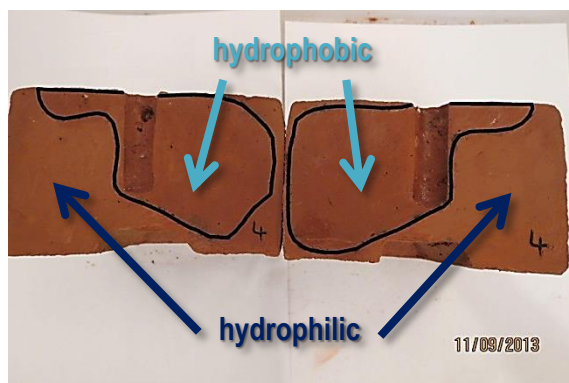


Figure 4: The spread of the injection application is too small / the bore hole distances are too wide / the spread of the injection agent is geometrically deformed, Source: Körber, P.

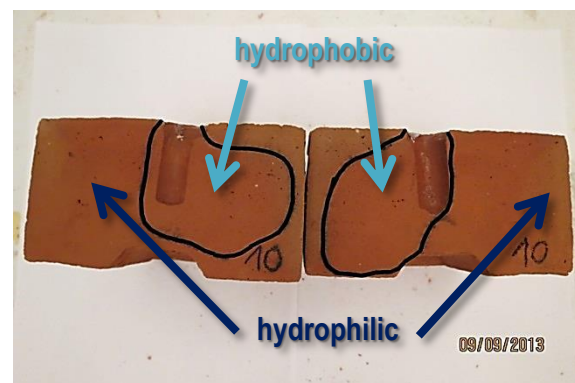
The injection agent use, discussed here, is applied at old buildings, in particular on monuments, but not in newly constructed structures. Here, the special factors that make up the use of injectables play a role as well. First, it is relevant that the injection application can only be used in capillary masonry. If the masonry consists, for example, of aerated concrete, an injection agent application is impossible because of the proportion of air pores. On the other hand, injection means for subsequent sealings can only be used in the load case 'non-pressing water' (soil moisture).

If the load case is 'pressing water', an injection agent sealing is excluded. Laboratory tests and experiments on objects have found that the deformed spread geometries are often based on the following causes:

- inhomogeneity of building materials: brick and mortar
- Cracks or cavities of the masonry
- Differences in the burning of the bricks
- Non-burned areas of brick
- Non-hydrated areas of mortar joints
- foreign matter / mixed masonry
- Moist differences in the masonry



a)



b)

Figure 5: a) & b) Brick after the injection, separated in the borehole area, the spread of the injection agent is geometrically deformed, Source: Körber, P.

3.1.1.2 To thesis 1

In the past, injectables for subsequent building waterproofing were often used without a masonry diagnostic, without knowledge of the environment and sometimes without sufficient knowledge of the injection agent to be used. The sealing success was rarely professionally controlled and just as rarely documented. It is the opinion of the processors that the proof of sealing success is not part of the contract. [57], [58], [59], [60], [61]

This effectively operates a synchronisation of all of the applicable injectables, the types of applications and the way the injection sealing is applied [62]. The masonry to be sealed in practice, however, is as diverse as the injection products that are available for the sealing. An accidental choice of an injection agent for use on an unknown masonry can only be successful at random. At present, around 150 different injection agents are available [62] for the subsequent masonry sealing [63].

Before an injection agent is selected for the subsequent sealing, the masonry to be renovated, the local conditions and the expected sealing success must first be considered and described in detail. In many cases, a cross-sectional sealing, consisting of injection means, is related to further redevelopment steps. Here it is crucial that all renovation measures are coordinated and that "in one system" can be worked [64], [65], [66].

The currently available detection methods for injections are based on long-term macroscopic measurements. Essentially, there are laboratory-based detection methods with test specimens produced on the laboratory, which are based on macroscopic investigations. These methods have a very long measurement time. In addition, the certification procedure according to WTA [66] exists. Since quasi-standard test specimens are used, this WTA- certification can only make statements about the basic effectiveness of an injection agent. In this respect, there is no detection method that can check the injection agent use on the object with fast and accurate results on the basis of small samples. However, recent scientific studies and publications have shown that, due to construction and building material anomalies, the results of the above-mentioned laboratory screening cannot readily be transferred to the use of injectables on a specific object. Frequently encountered masonry anomalies may be in cracks where any large quantities of the injection agent are discharged unplanned and thus the intended spread of the injection cannot be achieved. In addition, for years the literature pointed on the dangers of possible voids in the masonry. Another problem of the masonry to be treated is the moisture content. In this respect, it has already been proven that the borehole distances of borehole chains for the injecting agent application are not by no means always the same as those specified by the WTA leaflets [29], [30], [31], [32], [33], [34], [35], [36], [37].

In this context, there are correlations between the degree of the moisture content $[D(g)]$ of the masonry and the required distance of the boreholes. However, if one selects undifferentiated and without consideration of the degree of moisture, the distance between the boreholes currently recommended of the WTA [66], [78], the desired sealing success may not be achieved. The intended sealing area in the masonry is then simply fraught with flaws and island formations [67].

The successful use of an injection agent depends on the effectiveness of the agent itself, on its spread in the wall cross-section, on masonry anomalies, on any cracks and voids and on the degree of salification of the masonry. These old building-specific characteristics of the injection agent application cannot be determined by laboratory series investigations (like the WTA certification). Investigations are required on specimens collected on site from the building [67].

On the basis of the series of measurements carried out in this work, it has been proven that inject agents for the subsequent masonry sealing against capillary moisture does not have a broadband effect. This is partly due to the differences in masonry materials. On the other hand, not all injectables show the same effect on the different materials, in particular with respect to different degrees of moisture content. For these reasons, a quality control of the use of injectables is required during the application. In addition, a proof of the sealing success after completion of the injection work (in the finished state) on samples from the object is required. Due to the construction-accompanying quality control, fails in the injection work can be avoided and corrected in the early phase of the work. The final check serves to establish the achievement of the sealing goal.

3.1.2 **Thesis 2: As part of the use of injection waterproofing agents, a procedure is required to document the effectiveness of the application of the injection and to verify the extent to which the sealing goals have been achieved**

It has often been observed in the past with regard to the use of injectables that the causes for the lack of sealing success lies in the lack of analysis of the existing conditions of the sealing object and in the unqualified choice of the injection medium. Likewise, omissions regarding to the masonry diagnostics were occurred. As a result of a well-founded preparation, all available means for a subsequent sealing must be checked. In some cases, it may even be advisable to stop the use of injectables [68], [69]. Again, the required differentiated handling of the injection agents becomes clear. Condition analysis and masonry diagnostics, well-founded conception, as well as quality control and proof of effectiveness of the injection medium used must be contractually agreed. Only then these service components will be compulsorily remunerated as a benefit and the quality of the injection agent use will increase. According to thesis 1, there is a need to prove the quality of the injection agent used during and after the work. According to the current state of the art, injectables can be certified corresponding to the WTA leaflet [66], [78]. These processes are laboratory-worked off and operated by the manufacturers. Such certification confirms the basic efficacy of the injection agent under laboratory conditions. However, through this certification, there are no statements about the interactions of the injection agent with the specific local masonry.

The reasons for this are uncertainties due to inhomogeneities. In addition, cracks and cavities of the masonry play a role. Since such things often lie inside of the masonry, that is to say hidden, even a meticulous masonry diagnostics cannot name all the imponderables in advance. Since a subsequent sealing by injections often does not have the function of a sealing foil, it is necessary to name the sealing targets before starting the injection work. These sealing targets should be expressed in percentage as a measure of improvement. Based on these targets, the injection medium and the injection technology can be selected [57], [58], [59], [60], [61], [64], [65], [66].

The accompanying review of the injection work, required in this paper can serve as a corrective to the work which has already started. According to the intermediate results adjustments can be made on site. In this way, for example, the borehole distance could be adjusted. This approach comes close to the idea of a trial injection. However since such a procedure produces comparable intermediate and final results, the same analysis should be used as in the final check of the effectiveness of the used injectables. With the currently available detection methods, long-term moisture measurements are carried out on the object, which take years to complete. On the other hand, procedures are offered that need the creation of test specimens in the laboratory. These methods also require a long time course.

Ultimately, all currently available detection methods are equivalent to use injectables on specimens, which are built and tested for efficacy in the laboratory. With the current state of the art, the requirements for a detection method set out in this work, shown in 3.1.2.1., cannot be met.

After the injection work has been carried out, the sealing targets on the samples of the object must be qualified and checked differentiated. Therefore, a detection method is required which can demonstrate the geometric spread of the injection medium and the actually changed capillarity in the masonry. The detection method must be usable quickly, reliably and with low sample material expenditure both, during the work and as a follow-up.

3.1.2.1 Requirements for the new detection method

[29], [30], [31], [32], [33], [34], [35], [36], [37]

A detection method for checking the injection medium used on the specific object must be able to answer both, the question of the geometric spread of the injection medium and the question of the effectiveness of the agent within the sealing area. The requirements for the test matrix of this new proof method must follow the following parameters:

- The taking of a large number of samples must be possible
 - On-site sampling at any area of the masonry must be possible
 - Sampling during the injection work and after the injection work must be possible
 - Sample selection from the injection area must be possible
 - Reference samples on other masonry areas for verification must be possible
 - Low weight and small size of the individual samples must be possible
 - Simple minimally invasive sampling must be possible
 - Sampling in measuring axes at different depths of the masonry must be possible
- For accurate determination, a laboratory-based detection method is required
- The reproducibility of the measurement results must be given
- The measurement results must be objectifiable
- The measurement results must allow differentiated statements about the altered capillarity of the injection area
- The results must allow both qualitative and quantitative statements on efficacy of the injection
- The results must be available in short time intervals

3.1.3 **Thesis 3**: On the basis of scanning electron microscopic investigations in the ESEM, condensation processes on building materials on a microscopic scale can be generated, which can provide information about the capillarity of the building material being investigated

[69], [70], [71], [72], [73], [74], [75], [76], [77].

In the ESEM, the condensation processes can be observed in situ. The condensation water drops grow in a dynamic process. Images can be taken in the ESEM at any time during the ripening process. In this way contact angle measurements can be made on static and on dynamic drops.

The contact angle measurement is a well-studied tool for determining the degree of hydrophobia. This method is now to be applied to injection-treated, capillary masonry. To measure the contact angles in the ESEM, the 'Geometric Drop Contour Analysis' was developed in this work. In the context of this thesis, the studies in stage 2 prove that condensation processes in the ESEM can provide information about the capillarity of the investigated material. The ESEM is also suitable for determining the degree of hydrophily in the case that the ESEM cannot cause droplet formation due to the hydrophily of an examined sample. In this case the immediate formation of a water film can be exactly detected in the ESEM.

In the case of altered capillarity of the substance under investigation, on the one hand, a contact angle arises on the dewdrop deviating from the reference sample. In this way, the degree of change can be shown by the injection agent used. On the other hand, the contact angle measured in this way can be objectified by classifying the result according to existing definitions for the hydrophobia, shown in Fig. 1. [79], [80], [81], [82], [83], [84], [85].

3.1.3.1 ESEM condensation: hydrophilic properties => water film formation

In the following, examples of the condensation processes carried out in the ESEM on bricks and mortar samples are given by way of example. By way of illustration, condensation of hydrophilic, hydrophobic and superhydrophobic samples are also exemplified in 3.1.3.1 to 3.1.3.4. The medium supplied in the studies in the ESEM was water. Fig. 6 as an example shows a film forming out of a water film, that has been formed in the ESEM in the shortest possible time. It is a hydrophilic sample material with a contact angle of 0°. There is no droplet formation detectable.

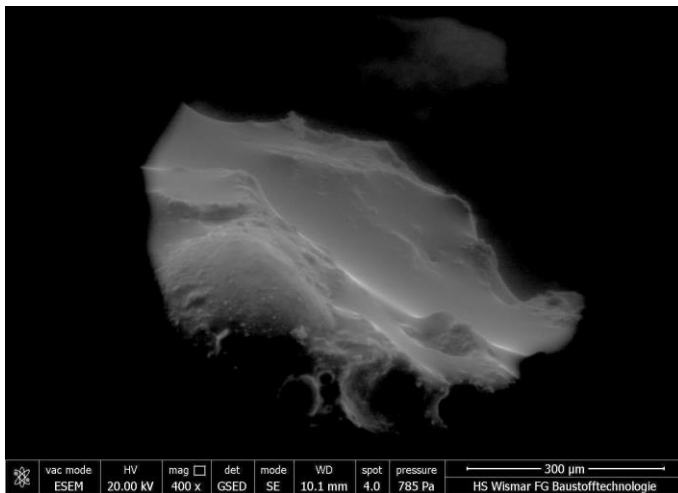


Figure 6:

Investigation in the ESEM: Brick, hydrophilic
=>instant water film forming
=>there is no droplet formation detectable
Source: Körber P.
[Attachment 01]

3.1.3.2 ESEM condensation: hydrophilic properties => Contact angle < 90°

Fig. 7 as an example shows a drop formation in the ESEM at a very flat angle. The drop angle is large enough to avoid an instant film formation, yet it is a hydrophilic contact angle, well below 90°.

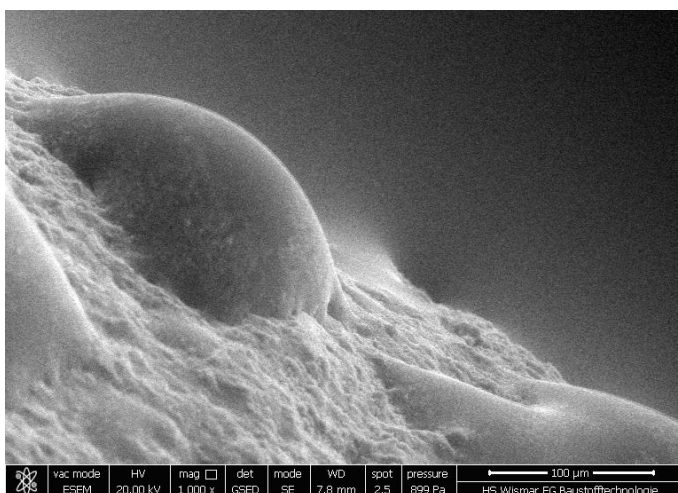


Figure 7:

Investigation in the ESEM: Brick hydrophilic
=>Contact angle well below 90°,
Source: Körber P.
[Attachment 02]

3.1.3.3 ESEM condensation: hydrophobic properties => Contact angle > 90°

In Figure 8 a drop formation with an angle > 90 ° is shown as an example. The drop shape and the contact angles prove that this is a hydrophobic sample. The contact angle is measured with the 'Geometric Drop Contour Analysis', see Fig. 11

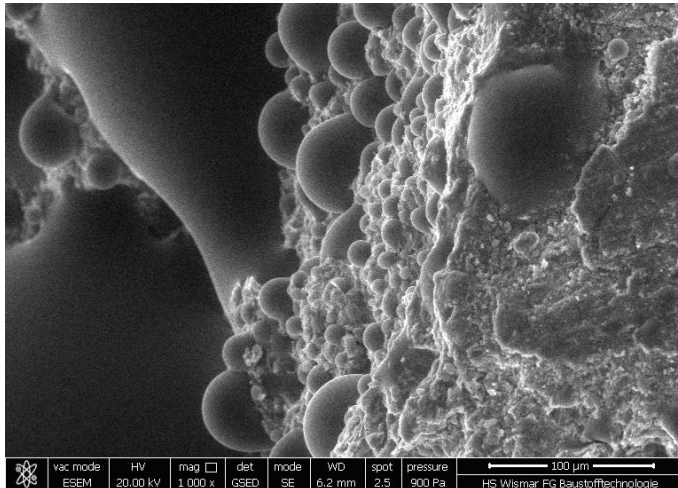


Figure 8:

Investigation in the ESEM: Brick hydrophobic
=>Contact angle well above 90°,
Source: Körber P.
[Attachment 03]

3.1.3.4 ESEM condensation: super hydrophobic properties => Contact angle > 150°

Fig. 9 as an example shows a spherical droplet formation. It is a superhydrophobic surface with a contact angle > 150 °.

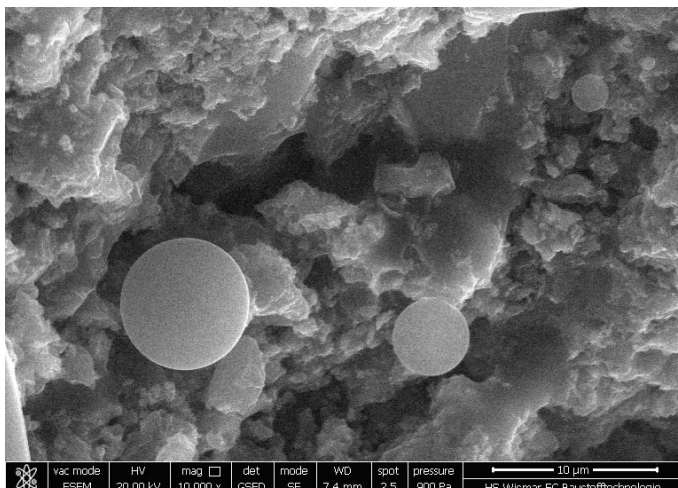


Figure 9:

Investigation in the ESEM: Brick, superhydrophobic
=>Contact angle > 150°,
Quelle: Körber P.
[Attachment 04]

3.1.3.5 ESEM condensation: Contact angle measurement with the 'Geometric Drop Contour Analysis'

The contact angle measurements in the ESEM take place in a three-dimensional space. Therefore, a geometrical model is required for the measurements. Similar to the drop contour method it is necessary to detect the contour of the drops. In the next step, a two-dimensional tangent measurement can be performed on the three-dimensionally detected drop. The contact angle measurement can be done directly in the ESEM or subsequently on images of the ESEM. In the ESEM, which in this case has a dynamic droplet formation, the mature drops must be measured. If a drop lies on the solid surface in such a way that there is a drop-side view, the contact angle of the drop can be measured directly in the ESEM or in the ESEM image, see Figure 10. If the drop lies on an oblique and rotated plane, then the drop is to see in a perspective. For such a case, the 'Geometric Drop Contour Analysis' in Figure 11 was developed in this thesis. The determination of the angle happens in the present case geometrically [44], [71], [83], [84].

To perform the 'Geometric Drop Contour Analysis', one makes use of the fact that a drop in its ideal form consists of a spherical segment. The contour of the spherical segment also corresponds in the perspective of the 2-dimensional contour of a spherical segment. The idealized sphere segment has a circular disk (= circle outline) as base area. If this circular outline is drawn perspective in the image created in the ESEM, then the circular arc intersects with the arc of the drop contour. The baseline can be plotted in the intersections of both bows. After the image is rotated and aligned with the baseline, the contact angle at the arc of the drop contour above the baseline can be measured 2-dimensionally in the tangent method. The 'Geometric Drop Contour Analysis' is based on an idealized model of the drop without a bump- effect and with idealizing the solid topography. Due to the idealization and due to the measurement tolerances, a tolerance must therefore be taken into account for this model. The tolerance of the 'Geometric Drop Contour Analysis' is set here to 3° . For the discussed proof method of the effectiveness of injection means a tolerance of 3° is appropriate and justifiable.

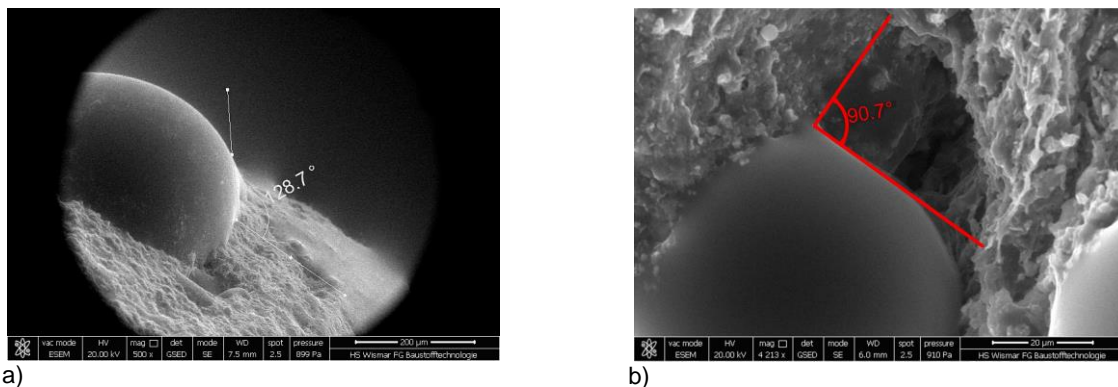


Figure 10: Direct measurement of the contact angle a) in the ESEM ($180^\circ - 128,7^\circ \Rightarrow 51,3^\circ$)
b) in the ESEM- Picture ($180^\circ - 90,7^\circ \Rightarrow 89,3^\circ$), Source: Körber P. [Attachment 05a,b]

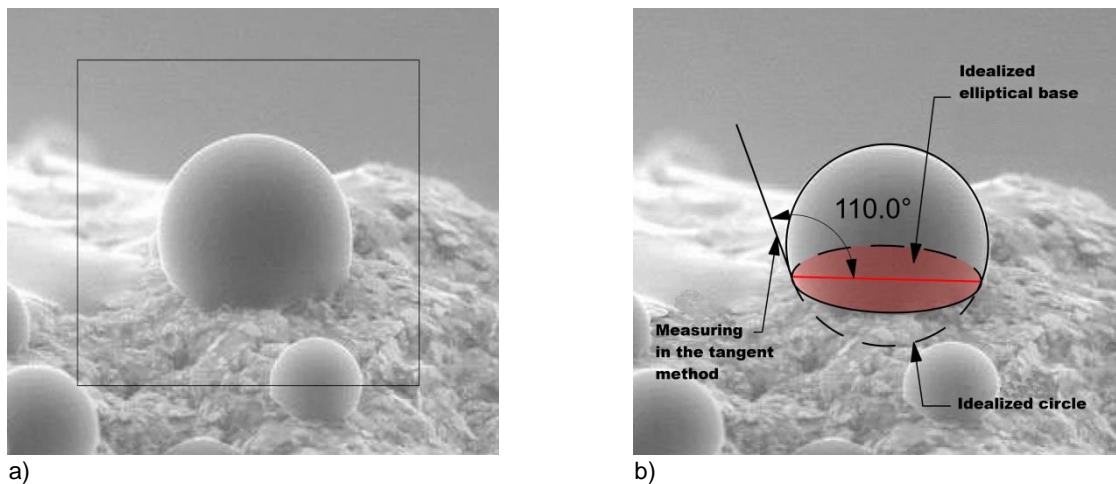


Figure 11: a) & b) ,Geometric Drop Contour Analysis' and the tangent measuring method,

Source: Körber P. [Attachment 06]

When measuring the contact angle in the ESEM, it is often necessary to measure at inclined levels. Therefore, there may be drops that have both an advancing and a retreating contact angle. First, the measurement must always be made on mature drops. A simplified model is used for the measurement in this work. In this model both contact angles (advancing and retreating angles) are measured. In the next step, both angles are added together and their sum is halved. In this way, the average contact angle is detected. In this idealized model it is assumed that the two angles deviate to the same extent (one negative and the other positive) from the possible undisturbed contact angle [44], [87], [88], [89].

3.1.4 **Thesis 4: Based on microscopic analyses of the contact angle in the ESEM, the altered capillarity of building materials, treated with injections can be detected. This detection method is suitable for construction practical use**

The detection method presented in this work can be used both during the construction process and after the work. By means of this method it is possible to differentiate the changed capillarity of the masonry qualitatively and geometrically. The detection method presented here fulfils the following criteria which are important for construction-practical use:

- It is possible to take a variety of samples
 - No test specimens need to be created
 - Sampling is possible in any masonry area
 - The sampling is minimally invasive, with mini- core- bores
 - The sampling is taking place in a depth-staggered measuring field
 - The sampling is taking place both, during the work and afterwards
 - Reference samples are taken to check the sealing targets
 - The samples are small in size, light in weight and easy to transport
 - In the ESEM, accurate results can be achieved in a short time
- The ESEM-based detection method allows exact and reproducible measurement results
- The measurement results can be objectified by previous macroscopic measurements
 - For this purpose, a database which is subdivided according to the individual injection means is to be created in advance. This data can be reused with each new ESEM measurement
- Based on the measurement results generated in the ESEM, both qualitatively and geometrically differentiated statements can be made about the altered capillarity

In this work, a two-stage laboratory test was performed on injection-treated samples. On 122 samples with different degrees of moisture, three waterproofing and pore narrowing injection agents were applied.

- In stage 1, the following macroscopic, conventional measurements were carried out on these samples:
 - Measurement of w- values
 - Measurement of water contents (as part of the w-value measurements)
 - Measurement of macroscopic contact angles in the Drop-Shape- Analyzer
 - Measurement of the spread of the inject agent
- In stage 1a, the following measurement procedures were performed on a selection from the stage 1 sample pool:
 - Measurement of RH- values* during the water absorption in a water bath up to measurement constancy
*RH = relative humidity
- In stage 2, the following measurement procedures were performed on the samples taken from the stage 1a (new samples out of the investigation areas of the samples of stage 1a):
 - Measurement of microscopic contact angles in the ESEM

Using mathematical modelling, the values measured in the ESEM (=stage 2) could be correlated with the macroscopic measurements of stage 1. With the help of this data, the obtained measurement results can be objectified and evaluated. The evaluation of the assigned w-values takes place according to Fig. 1 according to DIN EN 15148 and DIN EN 1062 T3 [15], [78].

3.1.4.1 Results of the investigations in stage 1

In Table 1 and 2 the examination results of stage 1 are listed. These measurement data were used to correlate them with the ESEM contact angles measured in stage 2. The following results are listed in stage 1:

- w-values [kg/m²√t]
- contact angles, macroscopic [°] [86]
- spread of the inject agent [mm]

MORTAR new					BRICK 2.0 ZDF new						
M	Samples MORTAR	D(t) [%]	W-Value [kg/m ² √t]	Contact angle [°] macroscopic	Spread of the inject agent [mm]	Z	Samples BRICK	D(t) [%]	W-Value [kg/m ² √t]	Contact angle [°] macroscopic	Spread of the inject agent [mm]
IA 1	M1	30	0.22	100	100	IA 1	Z1	30	0.04	116	100
IA 1	M2	50	0.3	95	100	IA 1	Z2	50	0.07	111	100
IA 1	M3	70	0.17	103	100	IA 1	Z3	70	0.10	108	100
IA 1	M4	90	0.33	90	100	IA 1	Z4	90	0.06	112	100
IA 1	M5	30	0.13	112	100	IA 1	Z5	30	0.06	112	100
IA 1	M6	50	0.15	109	100	IA 1	Z6	50	0.06	112	100
IA 1	M7	70	0.41	88	100	IA 1	Z7	70	0.05	113	100
IA 1	M8	90	0.46	84	100	IA 1	Z8	90	0.08	110	100
IA 2_PL	M9	30	0.33	95	100	IA 2_PL	Z9	30	0.08	108	100
IA 2_PL	M10	50	0.39	92	100	IA 2_PL	Z10	50	0.07	110	100
IA 2_PL	M11	70	0.87	50	100	IA 2_PL	Z11	70	0.12	105	100
IA 2_PL	M12	90	0.33	95	100	IA 2_PL	Z12	90	0.18	95	100
IA 2_PL	M13	30	0.17	103	20	IA 2_PL	Z13	30	0.05	113	100
IA 2_PL	M14	50	0.13	115	20	IA 2_PL	Z14	50	0.16	99	100
IA 2_PL	M15	70	0.43	85	20	IA 2_PL	Z15	70	0.09	106	100
IA 2_PL	M16	90	0.33	95	20	IA 2_PL	Z16	90	0.09	105	100
IA 2_P	M17	30	0.45	88	100	IA 2_P	Z17	30	0.11	100	100
IA 2_P	M18	50	0.45	88	100	IA 2_P	Z18	50	0.09	106	100
IA 2_P	M19	70	0.39	92	100	IA 2_P	Z19	70	0.07	110	100
IA 2_P	M20	90	0.3	95	100	IA 2_P	Z20	90	0.07	110	100
IA 2_P	M21	30	0.78	48	100	IA 2_P	Z21	30	0.11	99	100
IA 2_P	M22	50	0.48	85	100	IA 2_P	Z22	50	0.14	90	100
IA 2_P	M23	70	0.33	95	100	IA 2_P	Z23	70	0.07	110	100
IA 2_P	M24	90	0.26	105	100	IA 2_P	Z24	90	0.09	106	100
IA 3	M25	30	0.41	90	100	IA 3	Z25	30	0.56	66	0
IA 3	M26	50	0.24	99	100	IA 3	Z26	50	0.12	95	45
IA 3	M27	70	0.14	110	100	IA 3	Z27	70	0.49	70	0
IA 3	M28	90	0.2	107	100	IA 3	Z28	90	0.12	95	50
IA 3	M29	30	0.22	103	100	IA 3	Z29	30	0.05	113	50
IA 3	M30	50	0.13	115	100	IA 3	Z30	50	0.76	15	0
IA 3	M31	70	0.26	105	100	IA 3	Z31	70	0.67	43	0
IA 3	M32	90	0.17	108	100	IA 3	Z32	90	0.11	100	66
IA 3	M33	30	0.15	109	100	IA 3	Z33_A	30	0.05	115	
						IA 3	Z33_B	30	0.06	114	

Table 1:

Results of the investigations in stage 1 (macroscopic), part 1,
Source: Körber P.
[Attachment 07a]

BRICK						Composite masonry				
A	Samples BRICK	D(g) [%]	W-Value [kg/m ² √t]	Contact angle [°] macroscopic	Spread of the inject agent [mm]	V	Samples composite masonry	D(g) [%]	W-Value [kg/m ² √t]	Contact angle [°] macroscopic
IA 1	A2	50	0.82	60	100	IA 2_PL	V1_B	30	0.13	105
IA 1	A3	70	0.82	62	100	IA 2_PL	V1_C	30	0.19	101
IA 1	A4	90	0.21	120	100	IA 2_PL	V2_A	50	0.19	100
IA 1	A5	30	0.27	115	100	IA 2_PL	V2_B	50	0.45	88
IA 1	A6	50	0.27	115	100	IA 2_PL	V2_B	50	0.68	76
IA 1	A7	70	0.18	122	100	IA 2_PL	V3_A	70	0.33	95
IA 1	A8	90	1.14	30	100	IA 2_PL	V3_B	70	1.49	35
IA 2_PL	A9	30	0.24	118	100	IA 2_PL	V4_A	90	0.24	99
IA 2_PL	A10	50	0.2	121	100	IA 2_PL	V4_B	90	1.52	37
IA 2_PL	A11	70	0.27	116	100	IA 2_PL	V5	30	0.07	108
IA 2_PL	A12	90	0.28	115	100	IA 2_PL	V6_A	50	0.37	93
IA 2_PL	A13	30	0.27	116	100	IA 2_PL	V6_B	50	0.36	95
IA 2_PL	A14	50	0.35	105	100	IA 2_PL	V6_C	50	0.23	100
IA 2_PL	A15	70	0.29	110	100	IA 2_PL	V6_D	50	0.79	72
IA 2_PL	A16	90	0.27	116	100	IA 2_PL	V6_E	50	0.84	68
IA 2_P	A17	30	0.26	118	100	IA 2_PL	V7	70	0.14	110
IA 2_P	A18	50	0.16	123	100	IA 2_PL	V8_A	90	0.19	102
IA 2_P	A19	70	0.25	117	100	IA 2_PL	V8_B	90	0.2	100
IA 2_P	A20	90	0.24	118	100	IA 2_PL	V8_C	90	0.68	77
IA 2_P	A21	30	0.27	115	100	IA 2_PL	V9	90	1.89	15
IA 2_P	A22	50	0.28	114	100	IA 2_PL	V10	30	0.35	95
IA 2_P	A23	70	0.27	115	100					
IA 2_P	A24	90	0.24	118	100					
IA 3	A25	30	0.51	90	0					
IA 3	A26	50	1.25	25	0					
IA 3	A27	70	3.08	0	20					
IA 3	A28	90	1.48	12	20					
IA 3	A29	30	0.82	60	0					
IA 3	A30	50	1.17	35	20					
IA 3	A31	70	1.59	5	20					
IA 3	A32	90	1.26	27	0					
IA 3	A33	30	0.88	59						

Table 2:

Results of the investigations in stage 1 (macroscopic), part 2,

Source: Körber P.

[Attachment 07b]

As a result of the macroscopic investigations, the correlation between the w- values and the macroscopically measured contact angles are detected.

In the following diagram 2, the relations of macroscopically determined contact angles to the measured w- values, differentiating according to the individual injection means, are plotted as an example. In order to be able to classify the results, the hydrophobic and hydrophilic areas are shown in the diagram. The limit for the hydrophobicity is at a w- value of 0.5 kg / m²√t and at a contact angle of 90 ° [15], [78].

3.1.4.2 Evaluation of the macroscopic measurement results

Diagram 1 shows the w- values of the 122 injection-treated samples in a coordinated manner. The boundary between hydrophilicity and hydrophobicity is also w = 0.5 Kg / m²√t. The samples whose measured w- value is below the registered line for w = 0.5 Kg / m²√t can be described as hydrophobic according to Fig. 1 [15], [78]. Those samples, whose measured w-value is above this line, are called hydrophilic. As a result of the w-value measurements, it is found that the results of the samples M and Z are very predominantly in the hydrophobic region, irrespective of the particular injection medium and irrespective of the degree of moisture penetration.

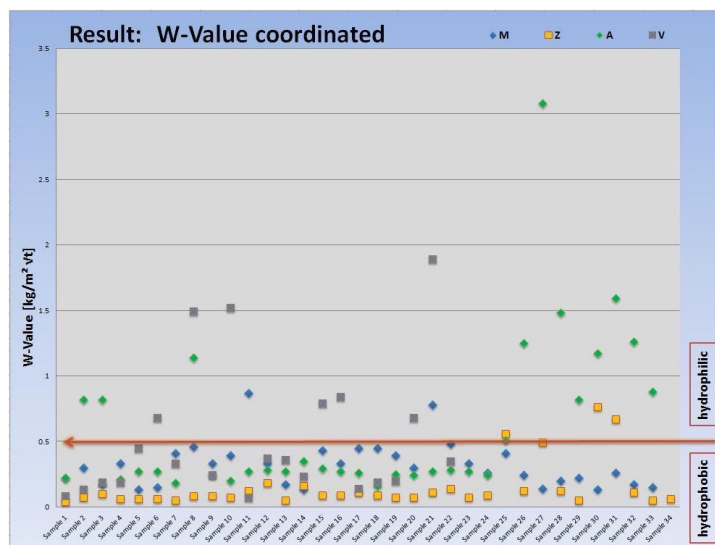


Diagram 1:

Results of all of the 122 w- values for the samples M, Z, A und V differentiated in hydrophobic und hydrophilic, Source: Körber P.

[Attachment 08]

Instead of that, the w-values of the samples A and V are very highly divided up into the hydrophilic area. The samples A and V (old- house- samples) are characterized by the already existing carbonation and a lower density. Diagram 2 shows the relationship between the measured macroscopic contact angles and the measured w- values, broken down by the individual injection means, as an example.

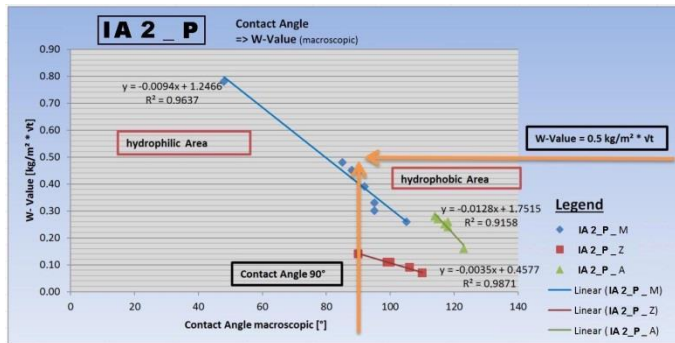


Diagram 2:

Applied injection IA 2_P (injection under pressure)
Relation between contact angle macroscopic and w-value macroscopic. Differentiated after the samples: M, Z and A.

The boundary between hydrophilicity and hydrophobicity, shown in Fig. 1, is defined with a contact angle of $\theta = 90^\circ$ and W-value $w = 0,5 \text{ Kg/m}^2\sqrt{t}$,
Source: Körber P. [Attachment 09]

In in the following diagram 3, the relation between the contact angle and the spread of the inject agent on the sample IA 3_Z, is shown as an example.

Concerning the borehole distances for the application of injections, usually the statements of the leaflet WTA 4-10-2015 [78] are used. These borehole distances are also cited in varied publications and in the technical literature as appropriate. In the leaflet WTA 4-10-2015 [78] one says that the boreholes should own the following horizontal distances for certificated injection means in the application in the bore process:

- 10 - 12.5 cm [78]

As a result of the investigation of this work it is shown in diagram 3, that the spread of the injection agent is mostly less than 50 mm. In diagram 3 only one sample has a spread of the agent of 70 mm. The spread of the inject agent does not reach the demands of the WTA leaflet [78]. The propagation of an inject agent in the building material stands in direct connection with the effectiveness of the injection. In a multitude of the specimens, examined here, the spread of the injection agent is in respect to the demands of the WTA [78] clearly too slightly. In this case the borehole- distances would have to be selected more slightly, to be able to guarantee a constant effectiveness of the injection. These results indicate that a detection procedure is required that can demonstrate the effectiveness of the injection, using samples from the treated masonry.

If this proof is carried out in an early phase of the injection work, the borehole distances may be selected more narrowly.

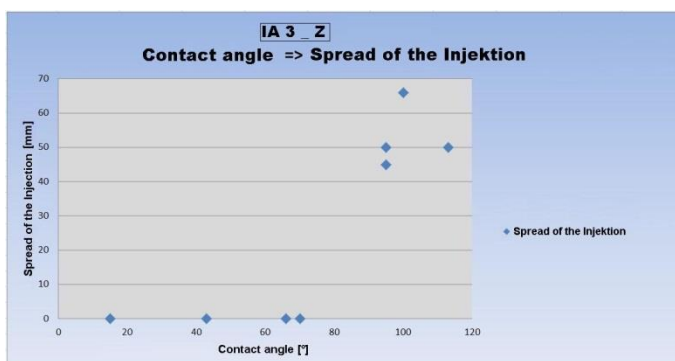


Diagram 3:

Applied injection IA 3_Z (injection without pressure)
Relation between contact angle macroscopic and the spread of the inject agent ,
Source: Körber P. [Attachment 10]

3.1.4.3 Investigations at stage 1a (RH- measurements)

At least 4 sensors each were attached to 5 selected samples in order to determine the relative humidity in the measuring chambers in the sample interior. The sensors were placed in drill holes and sealed airtight. The measuring chambers had a size of about 8 * 10 mm. The samples were adjusted analogously to the w-value determination in a water bath with a constant water level, so that the water absorption of the samples was carried out by capillary suction. The measurements were written until the value constancy by means of a data logger was achieved. The values for the relative humidity determined in this way describe the microclimate in the respective measuring chamber. The probes were deliberately placed both in the respective injection levels and in the non-hydrophobic areas. Subsequently, material samples were taken from the immediate vicinity of the measuring chambers. At these samples, the microscopic contact angles were determined in the ESEM.

3.1.4.4 Results of the data logger measurement at stage 1a

From the samples tested in stage 1, 5 samples were selected for the study which is described in step 1a. The measurement data was continuously written over periods of between 26 and 189 hours to the constancy of the measurement. To prepare the experiment, the samples were dried in the laboratory oven. Under the experiment, the water level in the water bath was kept consistently high. Diagram 5 shows the measured values of the data logger measurements up to the measurement constancy.

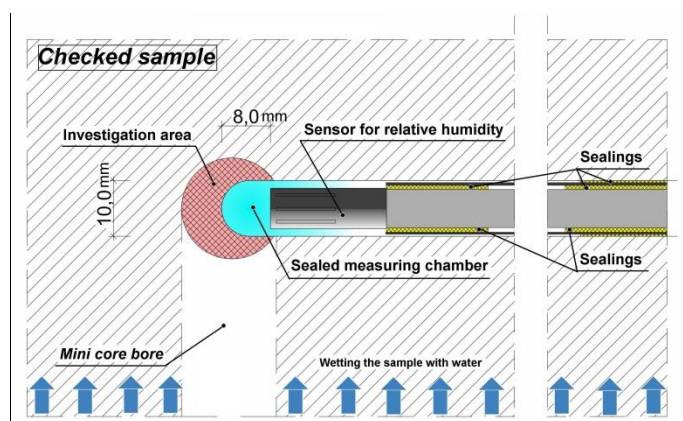


Figure 12:

Experiment setup data logger measurements

Source: Körber P.

[Attachment 11]

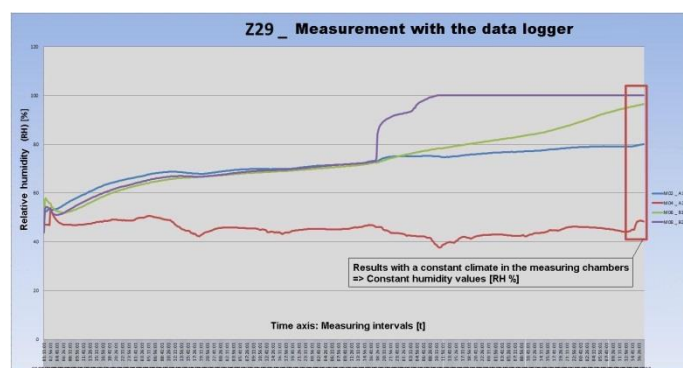


Diagram 4:

Results of the data logger measurements on the sample:

a) V5: RH values for 4 probes, period 26 hours

The red field marks the achievement of the measurement constancy,

Source: Körber P. [Attachment 12]

The samples taken from the adjoining areas around the measuring chambers for examination in the ESEM following the data logger measurements show very different measured values. This is due to the sample selection since they come specifically from the injection area as well as from supposedly non-hydrophobized areas. This method enables the simulation of conditions encountered in the proof procedure on site. In the application case the measuring axes of the sampling for the ESEM measurements can be staggered in their depth in the masonry. This way the measurement creates a spatial picture of the altered capillarity of the masonry.

3.1.4.5 Investigations in the ESEM at stage 2

In addition to the macroscopic w - values and the macroscopic contact angles, the measured relative humidity values serve to classify the microscopic contact angles, measured in the ESEM. Based on a mathematical model, the contact angles measured in the ESEM were assigned to w - values and fictitious moisture contents. The water contents only serve as fictitious quantities in the allocation of the measured w -values, which depends on the capillary water supply on site. With these fictitious water contents and the RH values a fictitious humidification can be simulated. The results of ESEM contact angles and RH measurements are shown in Table 15 [90], [91], [92], [93].

3.1.4.6 ESEM contact angles, correlated W -values, RH-values

In the following, the results of the data logger measurements in relation to the measured ESEM contact angles and the w - values determined from the mathematical modelling are shown in diagram 6. The border of the hydrophobicity is indicated by a w -value of $0.5 \text{ kg/m}^2\sqrt{t}$ and a contact angle of 90° [15], [78]. As a result, it is found that the RH- values and ESEM contact angles, expressed as linear functions, are exactly retrograde. The macroscopically determined and computationally modelled associated w -values, expressed as a linear function, are shifted parallel to the RH- values. This evaluation confirms the evidence of the detection method which is described here.

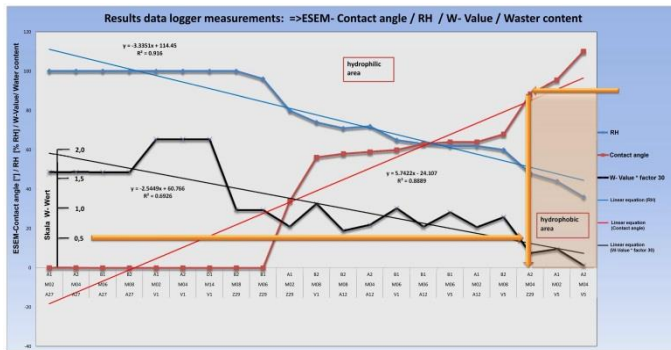


Diagram 5:

Result of the contact angle measured in the ESEM in relation to the data logger measurements and the macroscopic w values.

The border of hydrophobicity is defined as $\theta = 90^\circ$ and $w = 0.5 \text{ Kg} / \text{m}^2\sqrt{t}$

Source: Körber P. [Attachment 13]

3.1.4.7 Correlations to the ESEM- contact angles

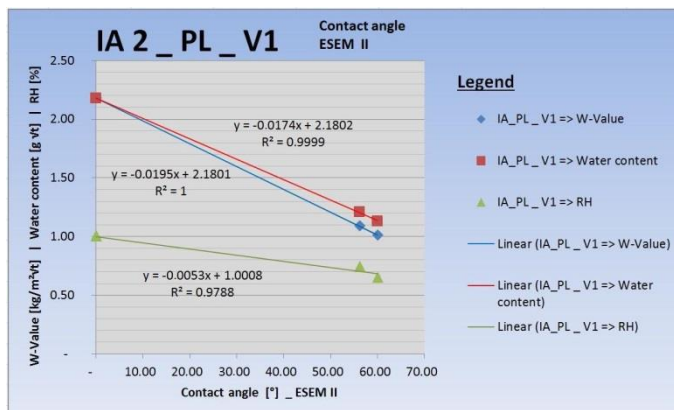


Diagram 6:

Inject agent IA 2_PL at the sample V1: Result of the contact angles measured in the ESEM in relation to the macroscopic w -values, the water contents and the RH-values

Source: Körber P.

[Attachment 14]

In Fig. 7 the ESEM-contact angle measurements are shown as an example in relation to the macroscopic w - values calculated in the mathematical modelling using linear functions. Besides the fictitious water contents are calculated, as well. The mathematical modelling of these data is calculated for each individual injection agent. As a result of this consideration, the slopes of the functions (here negative) are used to assess the extent to which congruences exist.

3.1.4.8 Mathematical modelling

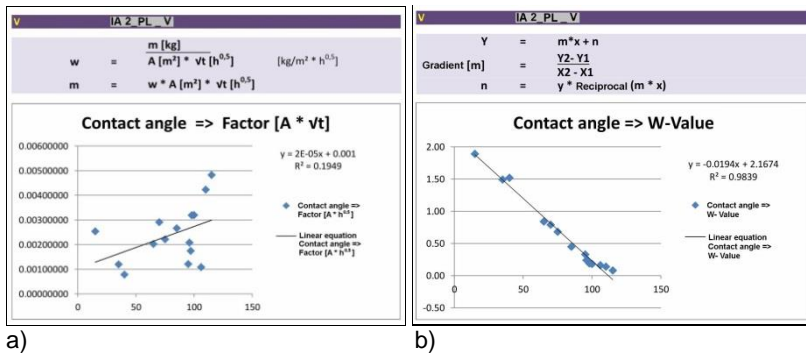


Figure 13:

a) & b): samples IA 2_PL_V:
relationships contact angle to
=> factor [A * sqrt(t)]
=> w value, macroscopic,
expressed in linear functions,
Source Körber P.
[Attachment 15]

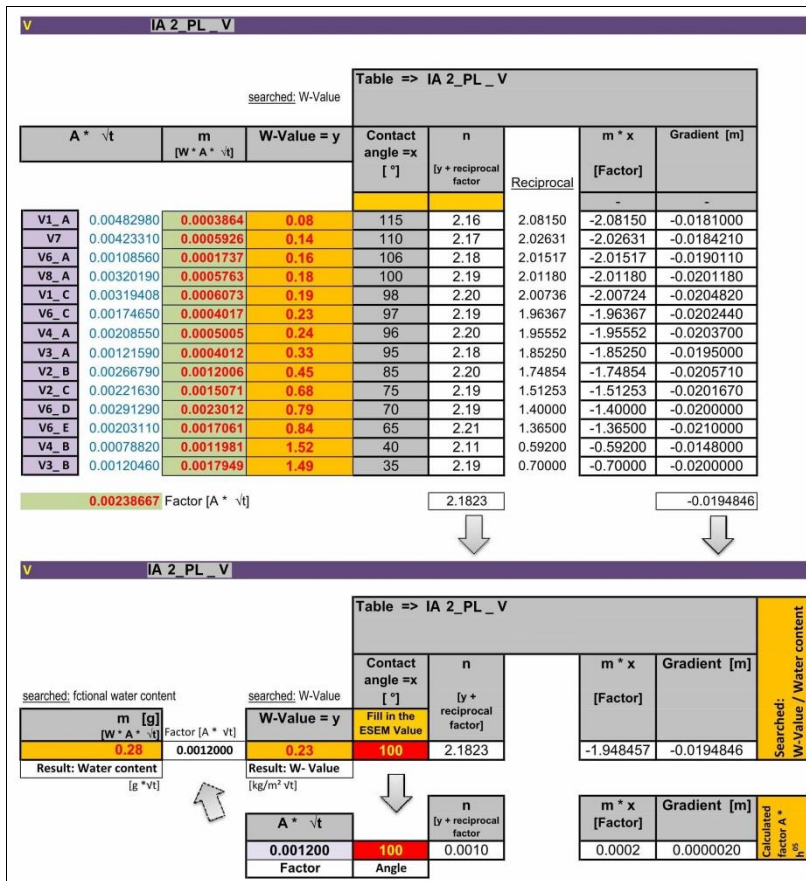


Figure 14:

Basis for the mathematical modelling
of w-values and fictitious water con-
tents associated with the measured
ESEM contact angles using the exam-
ple IA 2_PL_V,
Source: Körber P.
[Attachment 16]

For the mathematical modelling linear functions were used. Based on the data obtained in stage 1, factors for the relationship between macroscopic contact angles and macroscopic w-values as well as for the fictitious water contents can be determined, depending on the respective injection medium. In Fig. 13 and Fig. 14 it is shown the mathematical modelling as an example using the samples IA 2_PL_V.

With the data determined by the macroscopic tests in stage 1, w-values and fictitious water contents can be calculated and assigned for the contact angles measured in the ESEM. In this way, the contact angle measured in stage 2 in the ESEM can be correlated with the stage 1 data.

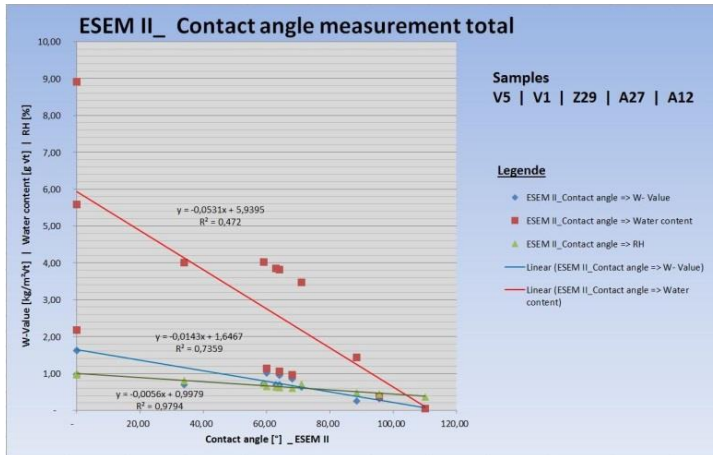


Diagram 7:

Relationships contact angle
=> w- value
=> fictitious water content
=> RH- value,
the entire ESEM measuring program is shown,
Source: Körber P.
[Attachment 17]

Measurement ESEM II

Sample	RH [%]	Contact angle		Water content	W-Value	Fill in the ESEM-Value	n	m * x	Gradient [m]
		ESEM measured value [°]	m [g] [W * A * t]						
[A 2_PL V5 M02 A1	44%	95.50	0.38	0.00119	0.32	95.50	2.1823	-1.8607793	-0.0194846
[A 2_PL V5 M04 A2	36%	110.00	0.05	0.00122	0.04	110.00	2.1823	-2.143306	-0.0194846
[A 2_PL V5 M06 B1	62%	64.00	1.06	0.00113	0.94	64.00	2.1823	-1.2470144	-0.0194846
[A 2_PL V5 M08 B2	60%	68.00	0.97	0.00114	0.86	68.00	2.1823	-1.3249528	-0.0194846
[A 2_PL V1 M02 A1	100%	-	2.18	0.00100	2.18	-	2.1823	0	-0.0194846
[A 2_PL V1 M04 A2	100%	-	2.18	0.00100	2.18	-	2.1823	0	-0.0194846
[A 2_PL V1 M06 B1	65%	60.00	1.13	0.00112	1.01	60.00	2.1823	-1.169076	-0.0194846
[A 2_PL V1 M08 B2	74%	56.20	1.21	0.00111	1.09	56.20	2.1823	-1.09503452	-0.0194846
[A 2_PL V3 M08 D1	100%	-	2.18	0.00100	2.18	-	2.1823	0	-0.0194846
[A 3 Z29 M02 A1	80%	34.00	4.00	0.00570	0.70	34.00	0.98	-0.2788	-0.0082
[A 3 Z29 M04 A2	48%	88.50	1.45	0.00570	0.73	88.50	0.057	0.0000	7.0E-19
[A 3 Z29 M06 B1	96%	-	5.59	0.00570	0.98	-	0.98	0	-0.0082
[A 3 Z29 M08 B2	100%	-	5.59	0.00570	0.98	-	0.98	0	-0.0082
[A 3 A27 M02 A1	100%	-	8.91	0.00550	1.62	-	1.62	0	-0.0125
[A 3 A27 M04 A2	100%	-	8.91	0.00550	1.62	-	1.62	0	-0.0125
[A 3 A27 M06 B1	100%	-	8.91	0.00550	1.62	-	1.62	0	-0.0125
[A 3 A27 M08 B2	100%	-	8.91	0.00550	1.62	-	1.62	0	-0.0125
[A 2_PL A12 M02 A1	62%	64.00	3.81	0.00550	0.69	64.00	1.23	-0.5376	-0.0084
[A 2_PL A12 M04 A2	72%	59.00	4.04	0.00550	0.73	59.00	1.23	-0.4956	-0.0084
[A 2_PL A12 M06 B1	63%	63.00	3.85	0.00550	0.70	63.00	1.23	-0.5292	-0.0084
[A 2_PL A12 M08 B2	71%	71.00	3.48	0.00550	0.63	71.00	1.23	-0.5964	-0.0084

Figure 15:

Mathematical determination of w-values and water contents belonging to the ESEM contact angles, complete stage 2 ESEM measurement program, source: Körber P.
[Attachment 18]

In diagram 8 it is shown the relationships between the ESEM contact angles and the calculated w-values, the calculated water contents and the measured RH-values. One can see the entire ESEM measuring program. The w-values express the altered capillarity of the material under investigation. With the fictitious water contents, a humidity simulation can be carried out in connection with the RH-values in the first stage of the detection method. With the help of this simulation, a three-dimensional image of a fictitious moistening of the examined masonry areas can be shown. In the case of application, the three-dimensional evaluation of the results is of great importance, as it can show the actual weak points of the new sealing level. Based on this simulation, the sealing target, expressed in an improvement percentage, can be questioned. In diagram 8 it can also be seen that the w-values, which lie below the mark $0.5 \text{ kg} / \text{m}^2 \sqrt{t}$, have a contact angle of more than 90° [15], [78]. In this respect, the border of hydrophobicity / hydrophilicity used here is consistent.

The second stage of the detection method is based on the evaluation via correlated w-values. These values can be assigned to the samples taken in graduated measuring axes. Here, a three-dimensional

image of the changed capillarity, which is based on the measurement program, is also arising. In Fig. 15 the calculated w-values and fictitious water contents for the entire stage 2 measurement program based on the ESEM contact angles are shown. The results for the w-values and the water contents were mathematically calculated by using linear functions.

3.1.4.9 Matrix of the new test procedure

In Fig. 16 the sequence of the test procedure in a matrix for clarification is indicated.

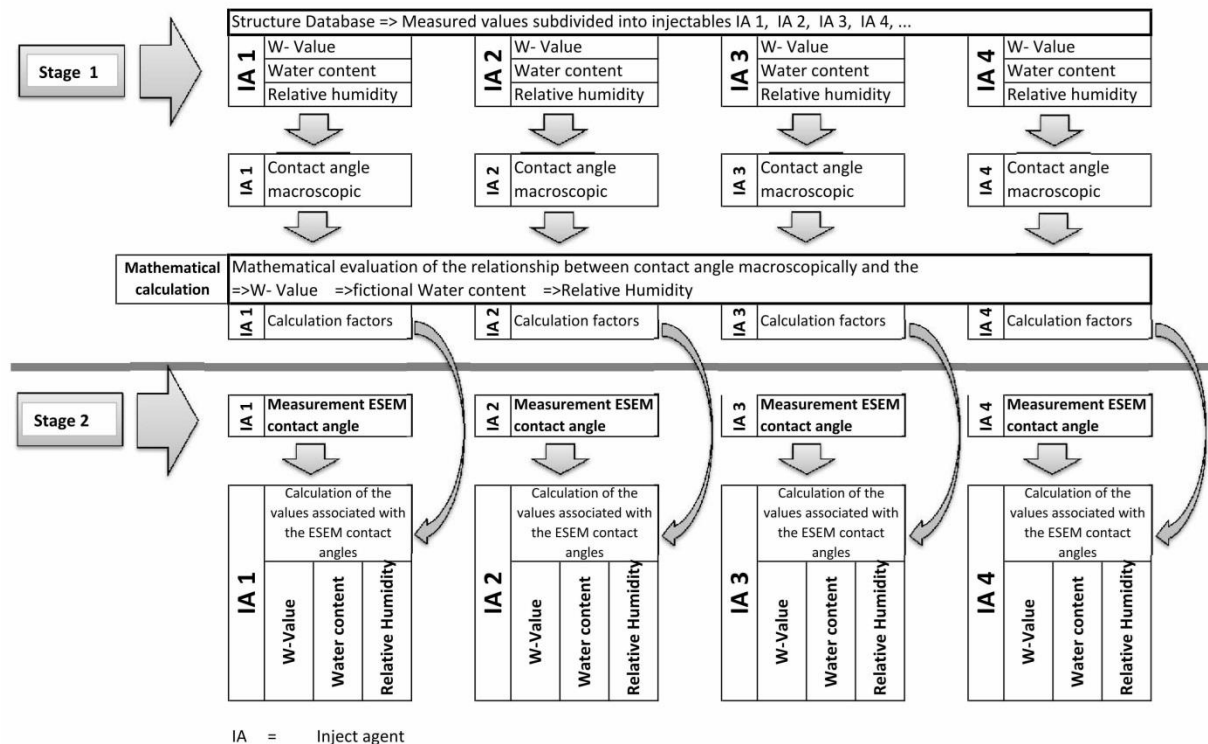


Figure 16: Matrix for the detection method presented in this work, Source: Körber P. [Attachment 19]

4. CONCLUSION, POSTGRADUATE RESEARCH INTERESTS

4.1 Conclusion

The new laboratory-based method for the detection of applied injection media, which is used for subsequent masonry sealing against rising damp, can demonstrate the altered capillarity of the masonry by means of imaging techniques in the ESEM. The measurement is carried out in the ESEM mode of the SEM by the dewing of samples that can be taken at the injection level and at reference points of the masonry. The capillarity of the building materials is detected by means of contact angle measurement on the dew drops produced in the ESEM [70], [71], [72], [73], [74], [75], [76], [77].

In the present series of tests, a total of 122 brick and mortar samples of various densities and different degrees of moisture penetration were treated with three different hydrophobic and capillary narrowing injection agents [94], [95], [96], [97].

In the first stage all samples were measured for macroscopic contact angles, w- values and fictitious water uptake. In the second stage the ESEM contact angles were determined to selected samples. A mathematical model was used to assign a w-value and a fictitious amount of water to each microscopic contact angle measured in the ESEM. These w- values can be used to evaluate the capillarity of the respective sample according to the test matrix in Fig. 1, based on DIN EN 15148 and DIN EN 1062 T3 [15], [78]. The fictitious water contents and the RH- values can be processed in a 3D-moisture simu-

lation. The new detection method for the effectiveness of injectables presented here has a practical advantage. It is understood as a further development of existing procedures. In contrast to existing detection methods, the proof procedure shown here, allows that samples obtained locally with the aid of mini core drillings being examined in the laboratory in a short time with a very small sample size. As a result, a qualitative, geometrically differentiated picture of the effectiveness of the injection can be shown on the basis of the detection method described here, both during the injection work and after the work. In this way, the actual spread of the injection agent in the masonry is geometrically demonstrated and the sealing success of the injection work can be confirmed. The accuracy of the detection method described here is $\pm 3^\circ$ with respect to the contact angles measured in the ESEM. Such accuracy is considered sufficient for the use described here as a method of detecting the effectiveness of injectables.

4.2 Postgraduate research interests

In order to correlate the contact angles measured in the ESEM, it will be necessary in the future to set up a database with macroscopically determined data, such as w-values, fictitious water contents and RH- values, differentiated according to the injection means. For the measurements as part of the database the use of a standard masonry in a laboratory is recommended. However, the individual injection agents and the degrees of moisture, as well as methods of injection are to be differentiated. As a result, w-values and fictitious water contents can be assigned to the contact angles measured in the ESEM according to the differentiation in compliance with the individual injection means. The values in the database can be reused for any similar ESEM measurement. With the results of the mathematical modelling, computer-assisted moisture simulations of the fictitious moisture penetration situation for the selected measuring field can be created in the future. The database can be used to prepare the ESEM contact angle measurements for relevant (commercially available) injection agents and the evaluation can quickly lead to results in the application case.

In the further development of the detection method presented here, in addition to the ESEM measurements, local contact angle rapid tests with handheld devices should be added in accordance with Fig. 17. In this way, additional rapid tests can be carried out on site. The results allow very early and very quick using computer-aided contact angle measurements for to estimate the sealing success. On the basis of such estimates, it is possible to react quickly to emerging error results by correcting the injection process. Appropriate devices are already available in the form of the Mobile Surface Analyzer, Fig. 17. [98]

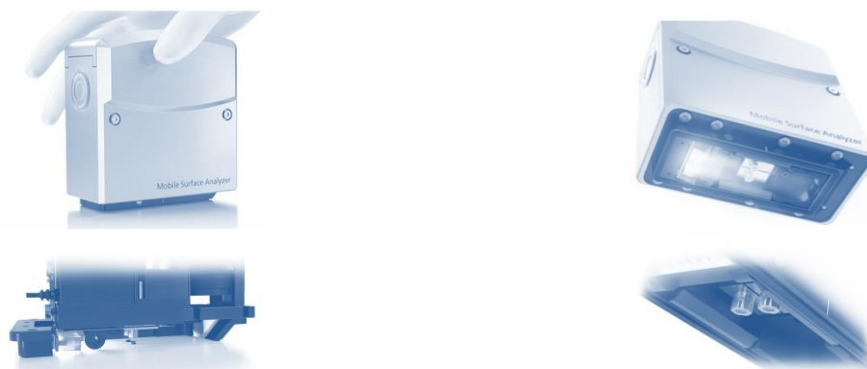


Figure 17: Local use of contact angle measurement using the Mobile Surface Analyzer,
Source: Krüss [Attachment 20]

In the further development of the proof method, presented here, the analysis of the contact angles measured in the ESEM can be carried out by means of a computer-aided tool in the future. There are software solutions in which the 3D- image- analysis leads to a higher accuracy of the contact angle to be measured. In this regard, it can be assumed that the accuracy of the contact angle measurement could be increased to $\pm 1^\circ$. [87], [88], [89]

1. Appendix

I. Publications of P. Körber in the context of this thesis

In connection with this PHD thesis Peter Körber published the following scientific articles:

No	Titel of the publication	Author	Co author	Year	Publisher
A	Injection agents for the subsequent horizontal sealing against capillary moisture transport The right injection medium for every case B + B, Bauen im Bestand	Körber, P.	Rupieper, D.	2013	Publishing company Rudolf Müller, Köln, Germany
B	Scanning electron micrographs of mortar and brick injectables, using condensation processes Energy supplier old buildings potentials, sustainability, object examples	Körber P.	Venzmer H.	2017	Publishing company Beuth, Berlin, Germany
C	Moisture protection in the old building renovation Missing subsequent building sealing in the masonry provokes consequential damage Der Bauschaden Spezial	Körber P.		2017	Publishing company Forum Herkert GmbH Merching, Germany
D	Mortar and brick materials treated with hydrophobic injection media, studied by Environmental Scanning Electron Microscopy	Körber P.		2018	Pollack Periodica Vol. 13, Hungary
E	Two-stage study program to demonstrate the effectiveness of injectables in masonry structures	Körber P.	Venzmer H.	2018	Edition Bautenschutz

II. References

- [1] Bonk, M. / Cziesielski, E., Lufsky, Bauwerksabdichtung, Bd. 7. Auflage, Vieweg + Teubner Verlag, 2010, p. XVII 609.
- [2] Klauß, S. / Kirchof, W., Altbaukonstruktionen- Materialien und U-Werte im Gebäudebestand: Baustoffe und Bauweisen mit regionalem Bezug, Fraunhofer IRB Verlag, 2010, p. 192.
- [3] Buss, H., Der Sachverständige für Schäden an Gebäuden. Handbuch für Ausbildung und Praxis, Fraunhofer IRB Verlag, Stuttgart, 2002, p. 331.
- [4] Deutscher Holz- und Bautenschutzverband e.V. DHBV, Handbuch der Bauwerksabdichtung: Normen, Regeln, Technik, Verlagsgesellschaft Rudolf Müller, Köln, 2009, p. 300.
- [5] Franke, L. / Schumann, I., Schadensatlas, Klassifikation und Analyse von Schäden an Ziegelmauerwerk, Fraunhofer IRB Verlag, Stuttgart, 1998, p. 172.
- [6] Frössel, F., Lehrbuch der Kellerabdichtung und -sanierung, Expert Verlag, Renningen, 2009, pp. 73-100.
- [7] Frössel, F., Mauerwerkstrockenlegung und Kellersanierung. Wenn das Haus nasse Füße hat, Fraunhofer IRB Verlag, Stuttgart, 2012, pp. 263-321.
- [8] Seele, J., Wasser- und Salztransport in Bauteilen - Schadensmechanismen und ihre Auswirkungen in Bauteilen, in *Feuchteschäden und Trockenlegung von historischen Bauten*, Bd. 12, Fraunhofer IRB Verlag, Stuttgart, 2004, pp. 53-63.
- [9] Moschig G., Bausanierung, Grundlagen-Planung-Durchführung, 3.Auflage, Vieweg + Teubner Verlag, Heidelberg, 2010
- [10] Stahr, M. u.a., Bausanierung, Erkennen und Beheben von Bauschäden, 6. Auflage, Springer Vieweg, Heidelberg, 2015, p. 991.

- [11] Moschig, G.F., Bausanierung, Grundlagen-Planung-Durchführung, Bd. 4. Auflage 2014, Springer Vieweg, Heidelberg, 2014, p. 459.
- [12] Stahr, M. (Hrsg), Bausanierung, Erkennen und Beheben von Bauschäden, 4. Auflage, Springer Vieweg, Heidelberg, 2009
- [13] Scholz, W. / Hiese, W. / Möhring, R. u.a., Baustoffkenntnis, Bd. Auflage: 18, Bundesanzeiger Verlag, Köln, 2016, p. 1058.
- [14] Hölzen, F.-J. / Weber, H., Abdichtungen von Gebäuden: Leitfaden für Neubau und Bestand, Auflage 2., Fraunhofer IRB Verlag, Stuttgart, 2014, p. 260.
- [15] Weber J., Horizontalsperren im Injektionsverfahren, in Weber J., Hafkesbrink V. (Eds.) Bauwerksabdichtung in der Altbausanierung: Verfahren und juristische Betrachtungsweise, Springer Vieweg, Wiesbaden 2012, pp. 205- 235.
- [16] Hölzen, F.-J. / Weber, H., Abdichtung von Gebäuden, Leitfaden für Neubau und Bestand, Fraunhofer IRB Verlag, Stuttgart, 2010, pp. 25-63, 146-167.
- [17] Altaha N., Ziegel Verblendmauerwerk, *Planung und Ausführung, Zweischalige Wand Marketing e.V. (Hrsg), Bonn, 2008*, Broschüre.
- [18] Ziegel Fibel, *Fakten über Ziegel, Ziegelsteine*, Mein Ziegelhaus GmbH & CoKG, Alzenau, 2007.
- [19] Deutsches Institut für Normung, „VOB Teil C DIN 18330 Maurerarbeiten“, Beuth Verlag, Berlin, 2006.
- [20] Honsinger D.J., „Abdichtung von erdberührten Bauteilen,“ *Der Bausachverständige*, 4/2015, pp. 9-15
- [21] Honsinger D.J., „Nachträgliche Abdichtung gegen kapillar aufsteigende Feuchte in Mauerwerk,“ *Der Bausachverständige*, 1/2013, pp. 23-32
- [22] Der Bauschaden Spezial, Feuchteschutz in der Altbausanierung, Forum Verlag Hekert, Merching, 2017, p. 200.
- [23] Akademie Bernhard Remmers, „Gebäudeinstandsetzung 10“, Ausgabe 2010, pp. 27-41 und 100-119
- [24] Bernhard Remmers Akademie, „Gebäudeinstandsetzung 12“, Ausgabe 2012, pp. 172-191
- [25] Bernhard Remmers Akademie, „Gebäudeinstandsetzung 13“, Ausgabe 2013.
- [26] Bernhard Remmers Akademie, „Gebäudeinstandsetzung 14“, Ausgabe 2014, pp. 70-73.
- [27] Bernhard Remmers Akademie, „Gebäudeinstandsetzung 15“, Ausgabe 2015.
- [28] Bernhard Remmers Akademie, „Gebäudeinstandsetzung 17“, Ausgabe 2017, pp. 32-35.
- [29] WTA Wissenschaftlich- Technische Arbeitsgemeinschaft für Bauwerkserhaltung und Denkmalpflege e.V., *Merkblatt 3-17*, Fraunhofer IRB Verlag, 2010, p. 18.
- [30] WTA Wissenschaftlich- Technische Arbeitsgemeinschaft für Bauwerkserhaltung und Denkmalpflege e.V., *Merkblatt 4-11-02/D*, Fraunhofer IRB Verlag, 2014, p. 20.
- [31] WTA Wissenschaftlich- Technische Arbeitsgemeinschaft für Bauwerkserhaltung und Denkmalpflege e.V., *Merkblatt 4-3-98/D*, Fraunhofer IRB Verlag, 1998, p. 14.
- [32] WTA Wissenschaftlich- Technische Arbeitsgemeinschaft für Bauwerkserhaltung und Denkmalpflege e.V., *Merkblatt 4-4-04/D*, Fraunhofer IRB Verlag, 2004, p. 21.
- [33] WTA Wissenschaftlich- Technische Arbeitsgemeinschaft für Bauwerkserhaltung und Denkmalpflege e.V., *Merkblatt 4-5-99/D*, Fraunhofer IRB Verlag, 1999, p. 16.
- [34] WTA Wissenschaftlich- Technische Arbeitsgemeinschaft für Bauwerkserhaltung und Denkmalpflege e.V., *Merkblatt 4-6-05/D*, Fraunhofer IRB Verlag, 2005, p. 24.
- [35] WTA Wissenschaftlich- Technische Arbeitsgemeinschaft für Bauwerkserhaltung und Denkmalpflege e.V., *Merkblatt 4-6-14/D*, Fraunhofer IRB Verlag, 2014.
- [36] WTA Wissenschaftlich- Technische Arbeitsgemeinschaft für Bauwerkserhaltung und Denkmalpflege e.V., *Merkblatt 4-7-02/D*, Fraunhofer IRB Verlag, 2002, p. 8.
- [37] WTA Wissenschaftlich- Technische Arbeitsgemeinschaft für Bauwerkserhaltung und Denkmalpflege e.V., *Merkblatt E 4-6-12/D*, Fraunhofer IRB Verlag, 2012, p. 32.
- [38] Gai, P.L., In-Situ Microscopy in Materials Research, Bd. 1, P. Gai, (Hrsg.), Springer Science+Business Media New York, 1997, pp. 336.
- [39] Gai P. L. / Boyes E. D., Environmental high resolution electron microscopy in materials science, In: Gai P. L. (Hrsg.) In-Situ Microscopy in Materials Research, Springer, Boston, 1997, pp. 123 -147.
- [40] Guikema, J.-W., *Scanning Hall Probe Microscopy of Magnetic Vortices in Very Underdoped yttrium-barium-copper-oxide*, Stanford Linear Accelerator Center, Stanford University, Stanford, 2004
- [41] Colliex Ch. Elektronenmikroskopie, Eine anwendungsbezogene Einführung, Wissenschaftliche Verlagsgesellschaft mbH, Stuttgart, 2008.
- [42] Reimer L., Pfefferkorn G. Raster- Elektronenmikroskopie, Springer Verlag, Berlin Heidelberg, 1977.
- [43] Eggert F. Standardfreie Elektronenstrahl-Mikroanalyse (mit dem EDX im Rasterelektronenmikroskop), Books on Demand, Norderstedt, 2005.
- [44] Yuan A. / Lee T. R., Contact angle and wetting properties, in Bracco G., Holst B. (Eds.), Surface Science Techniques, Springer Verlag Berlin Heidelberg, 2013, pp. 3- 34.
- [45] Krüss, Application Report AR244D, *Charakterisierung mikroskopische kleiner Oberflächen*, Hamburg, 2005.

- [46] Krüss, Application Report AR235D, Hamburg, 2003.
- [47] Krüss, Application Report AR 230D, *Charakterisierung von schmutzabweisenden Beschichtungen*, Hamburg, 2002.
- [48] Krüss, Application Report AR 229D, Contact angle measurement on large surfaces, Hamburg, 2002.
- [49] Bracco, G. / Holst, B. (Hrsg), *Surface Science Techniques*, Springer Verlag, Berlin, 2013, pp. 663.
- [50] Viel B., *Strukturiertes Kolloidpartikel für ultrahydrophobe, schmutzabweisende Oberflächen TU Darmstadt*, 2007, Dissertation.
- [51] Deutsches Institut für Normung, „DIN 15148 Bestimmung des Wasseraufnahmekoeffizienten bei teilweisem Eintauchen,“ Deutsches Institut für Normung e.V., Beuth-Verlag, Berlin, 2003.
- [52] Patitz G., „Anwendung zerstörungsfreier Verfahren zur Untersuchung alten Mauerwerks und alter Betonbauwerke,“ *Der Bausachverständige*, pp. 9-14, 3/2009, Der Bausachverständige.
- [53] Balak M./ Pech A., *Mauerwerkstrokenlegung*, Birkhäuser Verlag, Basel, 2017, p. 273
- [54] Venzmer, H., *Mauerwerkssanierung von A-Z; Fachbeiträge zu Diagnostik und Instandsetzung*, Bauwesen Verlag, Berlin, 2001, p. 560.
- [55] Frössel F., „Wunsch und Wirklichkeit bei der nachträglichen Horizontalabdichtung,“ in *Feuchteschäden und Trockenlegung von historischen Bauten*, Bd. 12, Fraunhofer IRB Verlag, Stuttgart, 2004, pp. 15-32.
- [56] Hölzen F.-J., „Praxisbeispiel einer ganzheitlichen nachträglichen Bauwerksabdichtung mit Systemgarantie,“ *Bausubstanz*, 1/2016 pp.44- 47
- [57] IFB Bauforschung, Institut für Bauforschung e.V., „Forschungsbericht: IFB-19568/2009; Untersuchung; Feuchteschäden durch fehlerhafte Bauwerksabdichtungen,“ Institut für Bauforschung e.V., Hannover, 2009, Forschungsbericht.
- [58] Künzel H., *Bauphysik und Denkmalpflege*, Fraunhofer IRB Verlag, Stuttgart, 2009, p. 148.
- [59] Künzel H., „Bauphysik- Geschichte(n) Nr. 17, Aufsteigende Feuchte: Großes Fragezeichen!,“ *ARCONIS 4/2002*, pp. 24-26
- [60] Körber, P., „Unterlassene Injektionsmittelabdichtung hat Folgeschäden, Hausschwamm durch fehlende nachträgliche Abdichtungen“, in *Der Bauschaden Spezial, Feuchteschutz in der Altbausaniierung*, Forum Verlag, Merching, 2017.
- [61] Lesnych, N. u.a. / Venzmer, H., „Dicht oder undicht? Tomografische Analytik von Injektionsmittel-Horizontal-abdichtungen an verschiedenen Objekten,“ in *Abdichten im Holz- und Bautenschutz: Normen, Regeln und Entwicklung*, Beuth-Verlag, Hrsg., B+B Forum Wismar, 2011, pp. 29-53.
- [62] Körber P. / Rupieper D., „Marktübersicht Injektionsmittel für die nachträgliche Horizontalabdichtung gegen kapillaren Feuchttransport,“ *B+B Bauen im Bestand*, 5. Ausgabe, 2013, pp. 54 - 60.
- [63] Appel, B. / Bertels, M. / Dahmen, P. / Engel, J. / Fischinger, R. / Fix, W. / Gänsmantel J. / Georgy, I. / u.a., *Praxis-Handbuch Bautenschutz: Beurteilen, Vorbereiten, Ausführen*, Rudolph Müller Verlag, Köln, 2012, p. 210.
- [64] Venzmer, H. / Schmidt, B. / Schmidt, D., (Hrsg), *Energielieferant Altbau, Potenziale/Nachhaltigkeit/Objektbeispiele*, Beuth Verlag, Berlin, 2017, p. 217.
- [65] Walter A. / Venzmer H., *Nachweis von Injektionsmitteln in mineralischen Baustoffen mittels Thermischer Analyse (TA)*, in Schmidt B., Schmidt D., Venzmer H., (Hrsg) *Energielieferant Altbau, Potenziale/Nachhaltigkeit/Objektbeispiele*, Beuth Verlag, Berlin, 2017, pp. 77- 84
- [66] Venzmer H./ Walter A., *Bautenschutz durch Abdichtung: Modellierung der Injektionsmittel-ausbreitung in mauerwerksbaustoffen*, in Venzmer H. (Ed.) *Bautenschutz: Innovative Sanierungslösungen*, Auflage 1, Beuth Verlag, Berlin, 2014, pp. 21–29.
- [67] Körber P./ Venzmer H. „Rasterelektronenmikroskopische Nachweise von Injektionsmitteln in Mörtel- und Ziegelstrukturen unter Nutzung von Betaungsvorgängen, in *Energielieferant Altbau*, B.Schmidt, D.Schmidt, H.Venzmer (Hrsg)“ Beuth Verlag, Berlin, 2017.
- [68] Wallasch, S., *Pathologie der Ziegelmauerwerke und keramischen Baustoffen*, in *Feuchteschäden und Trockenlegung von historischen Bauten*, Fraunhofer IRB Verlag, Stuttgart, 2004, pp. 65-74.
- [69] *Vereinigung der Landesdenkmalpfleger in der Bundesrepublik Deutschland, Feuchteschäden und Trockenlegung von historischen Bauten, Berichte zu Forschung und Praxis der Denkmalpflege in Deutschland*, Erstausgabe, 1. Auflage, Frauenhofer IRB, Verlag, Stuttgart, 2004, p. 79.
- [70] Hardt T. A., *Environmental SEM and Related Applications*, In: Rickerby D. G., Valdrè G., Valdrè U. (Eds.) *Impact of Electron and Scanning Probe Microscopy on Materials Research*, NATO Science Series (Series E: Applied Sciences) Vol. 364, Springer Netherlands, 1999, pp. 397-406.
- [71] Stelmashenko N. A. / Craven J. P./ Donald A. M./ Terentjev E. M. / Thiel B. L., *Topographic contrast of partially wetting water dropelts in environmental scanning electron microscopy*, *Journal of Microscopy*, Vol. 204, No. 2, 2001, pp. 172–183.
- [72] Danilatos, G.D., „Environmental Scanning Electron Microscopy,“ in *In-Situ Microscopy in Materials Research*, ESEM Research Lyboratory, Sydney, Australia, Springer Science+Business Media New York, 1997, pp. 13-44.
- [73] Stokes D.J. / Thiel B.L. / Donald A.M., „Dynamic secondary electron contrast effects in liquid systems studied by ESEM,“ *Polymers and Colloids, Department of Physics, University of Cambridge, UK*, 2000.
- [74] Rykaczewski K. / Scott J. H. J. / Fedorocv G., *Electron beam heating effects during environmental scanning electron microscopy imaging of water condensation on superhydrophobic surfaces*, *Applied Physics Letters*, Vol. 98, 2011, pp. 106- 109.
- [75] Doehne E./ Stuli C., *Applications of the environmental scanning electron microscope to conservation science*, *MRS Online Proceeding Library Archive, Symposium G - Materials Issues in Art and Archaeology II*, Vol. 185, 1990, pp. 23–29

- [76] Doehne E., ESEM development and application in cultural heritage conservation, In-Situ Microscopy in Materials Research, P. I. Gai (Ed.) Ch. 3, 1997, pp. 45 -62.
- [77] Miljkovic N. / Enright R. / Wang E., Modeling and optimization of superhydrophobic condensatation, Journal of Heat Transfer, Vol. 135, No. 11, 2013, paper No. HT-12-1145.
- [78] WTA Wissenschaftlich- Technische Arbeitsgemeinschaft für Bauwerkserhaltung und Denkmalpflege e.V., *Merkblatt 4-10-15/D*, 02/2015.
- [79] Hacquebord A./ Lubelli B./ Hees van R./ Nijland T., Evaluation of spreading and effectiveness of injection products against rising damp in mortar/brick combinations, *Procedia Chemistry*, Vol. 8, 2013, pp. 139–149
- [80] Tamas F./ Tuns I., Removing capillary moisture from brick walls using a drying method and case study, *Bulletin of the Transilvania University of Brasov, Series I: Engineering Sciences*, Vol. 3, No. 52, 2010, pp. 323–328.
- [81] Pop, M. / Campian C., *Methods for elimination of dampness in Building walls, IOP Conference Series: Material Science and Engineering 133*, 2016
- [82] Nenadálova S./ Balik L./ Kolisko J. / Klecka T., Impact of the chemical injection method on the dispersion of the injected agents in masonry, *Proceedings of the Conference on the Rehabilitation and Reconstruction of Buildings, CRRB 2012, Advanced Materials Research*, Vol. 688, 2012, pp. 73–78
- [83] Hecht, C. / Steiner, T., „Die Kontaktwinkelmessung für den Bausachverständigen,“ *Der Bausachverständige*, 2/2009, pp. 29-31
- [84] Herrmann, U./ Littmann, K. / Mengel, U., Hydrophobierungen - Über die Kunst, Wasser von mineralischen Baustoffen fernzuhalten, *Universität Hannover 3/4*, 2002, 68-71.
- [85] Unterdenweide, K. / Schmidt -Döhl, F., „Moderne Pysikalische Methoden bei Bauschadensuntersuchungen,“ *Der Bausachverständige*, 4/2009, pp. 12-16
- [86] Krüss, Drop Shape Analyzer - DSA25, Hamburg, 2018.
- [87] Krüss, Technical Note TN312D, *Praxis der Kontaktwinkelmessung*, Hamburg, 2007.
- [88] Krüss, ADVANCE Software, *Software*, Krüss, Hrsg., Hamburg, 2018.
- [89] Krüss, *Schulung / Theorie _ Glossar _ Kontaktwinkel*, Hamburg, 2017.
- [90] Harten, U., *Physik Einführung für Ingenieure und Naturwissenschaftler*, Springer Vieweg, Berlin Heidelberg, 2014, pp. 369.
- [91] Kamps, S., *Untersuchungen u. Herstellung von hydrophoben und superhydrophoben Beschichtungen zur Verbesserung des Wärmeübergangs durch dauerhafte Tropfenkondensation*, TU Darmstadt, 2012, Dissertation, p.149
- [92] Dufek M., FEI Company, *The Quanta FEG 450 , SEM / ESEM User Operation Manual*, 2013, p.7-88
- [93] Fischer T., FEI, *Quanta FEG 450*, T. Fisher (Hrsg.), 2013.
- [94] Neisius Bautenschutzprodukte, *CavaStop300*, K. Neisius Bautenschutzprodukte (Hrsg.), Kühlungsborn, 2009, Merkblatt.
- [95] Remmers Baustofftechnik GmbH, *Technisches Merkblatt Produkt-Nr. 1810, Kiesol, Lönningen*, 2008, Merkblatt
- [96] Köster Abdichtungssysteme, *Köster Crisin 76 Konzentrat*, K. Abdichtungssysteme, Hrsg., Aurich, 2015 Technisches Merkblatt M 279.
- [97] Köster Abdichtungssysteme, *Horizontalsperren gegen aufsteigende Feuchtigkeit*, Technisches Merkblatt , Köster Bauchemie (Hrsg), Aurich, 2015, Merkblatt
- [98] Krüss, *Mobile Surface Analyzer - MSA*, KRÜSS, Hrsg., Hamburg, 2018 Broschüre.

III. List of Figures

Figure 1: Evaluation matrix of the results of the W-Value measurements, based on DIN EN 15148 and DIN EN 1062 T3	3
Figure 2: Application spread and borehole distances are ideal: => overlapping cylindrical spread	4
Figure 3: The spread of the injection application is to small / borehole distances are to far.	5
Figure 4: The spread of the injection agent is geometrically deformed.	6
Figure 5: a) & b) Brick after the injection: The spread of the injection agent is geometrically deformed.....	6
Figure 6: Investigation in the ESEM: Brick, hydrophilic =>instant water film forming =>there is no droplet formation detectable.....	10

Figure 7: Investigation in the ESEM: Brick hydrophilic =>Contact angle well below 90°	10
Figure 8: Investigation in the ESEM: Brick hydrophobic =>Contact angle well above 90°	11
Figure 9: Investigation in the ESEM: Brick, superhydrophobic =>Contact angle > 150°	11
Figure 10: Direct measurement of the contact angle a) in the ESEM (=>51,3°) b) in the ESEM- Picture (=>89,3°).....	12
Figure 11: a) & b) ,Geometric Drop Contour Analysis' and tangent measuring method.....	13
Figure 12: Experiment setup data logger measurements.....	17
Figure 13: a) & b): IA 2_PL_V: relationships contact angle to => factor $[A * \sqrt{t}] => w$ value, macroscopic, expressed in linear functions.....	19
Figure 14: Basis for the mathematical modelling	19
Figure 15: Mathematical determination: complete stage 2 ESEM measurement program	20
Figure 16: Matrix for the detection method presented in this work.....	21
Figure 17: Local use of contact angle measurement using the Mobile Surface Analyzer	22

IV. Table list

Table 1: Results of the investigations in stage 1 (macroscopic), part 1	14
Table 2: Results of the investigations in stage 1 (macroscopic), part 2.....	15

V. Diagram directory

Diagram 1: Results of all of the 122 w- values for the samples M, Z, A und V differentiated in hydrophobic und hydrophilic.....	15
Diagram 2: IA 2_P: Relation between contact angle macr. and w-value macr., differentiated after the samples: M, Z and A	16
Diagram 3: IA 3_Z: Relation between contact angle macroscopic and the spread of the inject agent	16
Diagram 4: Results of the data logger measurements on the sample a) V5: RH values for 4 probes, period 26 hours.....	17
Diagram 5: Result of the contact angle measured in the ESEM.....	18
Diagram 6: Inject agent IA 2_PL at the sample V1: Result of the contact angles measured in the ESEM.....	18
Diagram 7: Relationships contact angle => w- value => fictitious water content => RH- value	20

VI. Consultations

Supervisor 1: Dr. habil. Erzsébet Szeréna Zoltán, University of Pécs, Marcell Breuer Doctoral School
associate professor

Supervisor 2: Dr. Adél Len, University of Pécs, Marcell Breuer Doctoral School, assistant professor

VII. Statutory declaration

I declare under oath that I have made this dissertation work autonomously. The from other sources taken directly or indirectly thoughts or formulations are designated as such. The work has not been presented at any other educational institution, and is not yet published.

Springe / Pécs, _____

Peter Körber M.Sc.

VIII. Note of thanks

For the use of the laboratory of the University of Wismar, Faculty of Engineering, I would like to expressly thank Prof. Dr. Malorny and Dr. Barfels.

In particular, I would like to thank the initiator of the Doctoral College at the University of Wismar and the Master- Program Building Protection of the WINGS, Prof. Dr. Dr. habil. H. Venzmer.

Finally, I would like to thank my family for the patience I have received during my work.

IX. Curriculum vitae

Personal data

Name: Peter Körber
Date of birth: 12.03.1966
Place of birth: Hannover, Germany
Nationality: German
E-mail: kontakt@architekt-koerber.de

Completed vocational training:

1984 - 1986 Training as carpenter, Hannover, Germany
1986 Journeyman carpenter

Completed higher education / Professional career:

1988 - 1992 Study course architecture, University HAWK Hildesheim, Faculty of architecture
1992 Dipl. Ing. Architect
1994 Member of the Chamber of Architects, Lower Saxony, Germany
2003 Public appointment and swearing as an expert of damage to buildings
2005 Foundation: Engineering- and Expert Office Körber
2008 Public appointment and swearing as a valuer of buildings and properties
2010 TEGoVA Recognised European Valuer, REV
2011 - 2014 Study course building protection, University of Wismar, Faculty of Engineering
2014 Master of Science M.Sc., Engineer of building protection
2013 Member of the Chamber of Engineers, Lower Saxony, Germany
2013 Consulting engineer, Chamber of Engineers, Lower Saxony, Germany
2014 - 2018 Ph.D.
University of Wismar, Faculty of Civil Engineering, Doctoral College
University of Pécs, Faculty of Engineering and Information Technology,
Breuer Marcell Doctoral School

2. List of attachments

- Attachment 01: Figure 6: ESEM, Brick, hydrophilic
 - =>instant water film forming =>there is no droplet formation detectable

- Attachment 02: Figure 7: ESEM, Brick, hydrophilic
 - =>Contact angle well below 90°

- Attachment 03: Figure 8: ESEM, Brick, hydrophobic
 - =>Contact angle well above 90°

- Attachment 04: Figure 9: ESEM, Brick, superhydrophobic
 - =>Contact angle well above 150°

- Attachment 05a: Figure 10 a):
 - Direct measurement of the contact angle a) in the ESEM

- Attachment 05b: Figure 10 b):
 - Measurement of the contact angle b) in the ESEM- picture

- Attachment 06: Figure 11 b): Geometric Drop Contour Analysis

- Attachment 07a: Table 1:
 - Results of the investigations in stage 1 (macroscopic), part 1

- Attachment 07b: Table 2:
 - Results of the investigations in stage 1 (macroscopic), part 2

- Attachment 08: Diagram 1:
 - Results of all of the 122 w- values for the samples M, Z, A und V

- Attachment 09: Diagram 2:
 - IA 2_ P =>Relation between contact angle macroscopic and w-value

- Attachment 10: Diagram 3:
 - IA 3_ Z =>Relation between contact angle and the spread of the inject agent

- Attachment 11: Figure 12: Experiment setup data logger measurements

- Attachment 12: Diagram 4: Sample V5, RH values for 4 probes, period 26 hours
- Attachment 13: Diagram 5: Result of the contact angle measured in the ESEM
- Attachment 14: Diagram 6: Inject agent IA 2_PL at the sample V1:
 - Result of the contact angles measured in the ESEM
- Attachment 15: Figure 13: a) & b): IA 2_PL_V: relationships contact angle to
 - => factor $[A * \sqrt{t}]$ => w value, macroscopic, expressed in linear functions
- Attachment 16: Figure 14: Basis for the mathematical modelling
- Attachment 17: Diagram 7: Relationships contact angle
 - => w- value => fictitious water content => RH- value
- Attachment 18: Figure 15: Mathematical determination:
 - complete stage 2 ESEM measurement program
- Attachment 19: Figure 16: Matrix for the detection method presented in this work
- Attachment 20: Figure 17: Local use of the Mobile Surface Analyzer



UNIVERSITY OF PÉCS _ BREUER MARCELL DOCTORAL SCHOOL
FACULTY OF ENGINEERING AND INFORMATION TECHNOLOGY

HOCHSCHULE WISMAR UNIVERSITY OF TECHNOLOGY, BUSINESS AND DESIGN
FACULTY OF ENGINEERING

PHD - THESIS

PETER KÖRBER

